[RADIOCARBON, VOL. 40, NO. 3, 1998, P. 1041–1083]

INTCAL98 RADIOCARBON AGE CALIBRATION, 24,000–0 cal BP

MINZE STUIVER,[1] PAULA J. REIMER,[1] EDOUARD BARD,[2] J. WARREN BECK,[3] G. S. BURR,[3] KONRAD A. HUGHEN,[4] BERND KROMER,[5] GERRY McCORMAC,[6] JOHANNES VAN DER PLICHT[7] and MARCO SPURK[8]

ABSTRACT. The focus of this paper is the conversion of radiocarbon ages to calibrated (cal) ages for the interval 24,000–0 cal BP (Before Present, 0 cal BP = AD 1950), based upon a sample set of dendrochronologically dated tree rings, uranium-thorium dated corals, and varve-counted marine sediment. The ^{14}C age–cal age information, produced by many laboratories, is converted to $\Delta^{14}C$ profiles and calibration curves, for the atmosphere as well as the oceans. We discuss offsets in measured ^{14}C ages and the errors therein, regional ^{14}C age differences, tree–coral ^{14}C age comparisons and the time dependence of marine reservoir ages, and evaluate decadal *vs.* single-year ^{14}C results. Changes in oceanic deepwater circulation, especially for the 16,000–11,000 cal BP interval, are reflected in the $\Delta^{14}C$ values of INTCAL98.

INTRODUCTION

The radiocarbon age time frame has been used extensively during the past 50 years in many disciplines. Because uncorrected ^{14}C ages and calibrated (cal) ages differ in a time-dependent fashion, the conversion of ^{14}C ages to cal ages is especially important for improving the validity of time estimates. Participants at the 16th International Radiocarbon Conference at Groningen (16–20 June 1997) discussed and recommended an update of previous calibration publications (Stuiver and Kra 1986; Stuiver, Long and Kra 1993). Following the advice of the international radiocarbon community, we present here an extended ^{14}C calibration data set, INTCAL98, that caps the 20th century ^{14}C age calibration efforts.

Dendrochronology provided the cal ages of the wood used for ^{14}C dating; their accuracy is established through standard dendrochronological checks and counterchecks for double or missing tree rings. The Irish oak (Pilcher *et al.* 1984) and the German oak and pine chronologies (Spurk *et al.* 1998) play a crucial role. The German oak chronology provides absolute counts of dendroyears back to *ca.* 10,300 cal BP. ^{14}C matching of the latest part of a floating German pine chronology to the earliest absolutely dated German oak extends this chronology to 11,857 cal BP. Errors in the matching may amount to 20 cal years (Kromer and Spurk 1998).

Uranium-thorium (U-Th) dating of corals extends the cal age range (Bard *et al.* 1998; Burr *et al.* 1998; Edwards *et al.* 1993). Whereas tree-ring ^{14}C, *via* the photosynthetic cycle, equilibrates with atmospheric carbon dioxide, corals equilibrate with mixed-layer ocean bicarbonate. The slightly lower ^{14}C activity (per gram of carbon) of the mixed layer, relative to the atmosphere, results in an offset (the ^{14}C reservoir age correction) between "atmospheric" and "oceanic" ^{14}C ages of samples with identical cal age. The reservoir correction (509 ± 25 ^{14}C yr over the 12,000–10,000 cal BP interval) was fixed by comparing Early Holocene tree-ring and coral ^{14}C activities of contemporaneous samples. Adding coral results extends the calibration curve to 24,000 cal BP. Although only two

[1]Quaternary Isotope Laboratory, University of Washington, Seattle, Washington 98195-1360 USA
[2]CEREGE, Europôle de l'Arbois, B.P. 80, 13545 Aix-en-Provence Cedex 4, France
[3]Physics Department, University of Arizona, Tucson, Arizona 85721-0081 USA
[4]Department of Earth and Planetary Sciences, Harvard University, Cambridge, Massachusetts 02138 USA
[5]Heidelberger Akademie der Wissenschaften, Im Neuenheimer Feld 366, D-69120 Heidelberg, Germany
[6]Radiocarbon Laboratory, The Queen's University, Belfast BT7 1NN, Northern Ireland
[7]Centrum voor Isotopen Onderzoek, Rijksuniversiteit Groningen, Nijenborgh 4, 9747 AG Groningen, The Netherlands
[8]Universität Hohenheim, Institut für Botanik–210, D-70593 Stuttgart, Germany

coral measurements exist for the 40,000–24,000 cal BP interval (Bard *et al.* 1998), they seem to point towards increasing differences between ^{14}C and cal ages.

Terrestrial varve chronologies, to be discussed in a future issue of *RADIOCARBON*, have not been used for construction of INTCAL98. A floating marine varve chronology, however, was used to strengthen the coral information from the 14,500–11,700 cal BP interval. To fix absolute time, the younger varve ^{14}C ages were matched with tree-ring ^{14}C ages (normalized on marine ^{14}C level).

Decadal wood samples were emphasized in *RADIOCARBON*'s 1986 and 1993 calibration issues. The ^{14}C content of a 10-yr wood sample, however, is not necessarily a perfect reflection of the atmospheric ^{14}C level of that decade. Tree-ring ^{14}C does not represent the seasons equally because a major portion of the wood is formed in spring and early summer. Tree-ring thickness also differs from year to year, causing variable annual ^{14}C contributions to the decadal average.

Decadal results were used in 1986 and 1993 for the construction of a (mostly) decadal Seattle calibration curve (Stuiver and Becker 1986, 1993). Combining these results with those obtained by Belfast for bidecadal samples led to a 20-yr calibration curve which has until now been used for most age calibrations (Pearson and Stuiver 1993; Pearson, Becker and Qua 1993; Stuiver and Reimer 1993).

Many ^{14}C ages have been determined on dendrodated wood covering only a couple of years. Instead of disregarding these high-precision measurements, we used a different approach for the INTCAL98 calibration curve. INTCAL98 "decadal" ^{14}C is obtained by averaging full-decadal and part-decadal (single- or multiple-year) results. ^{14}C ages of samples covering 20 yr also are included by allocating to each decade the bidecadal age with a standard deviation (σ) multiplied by 1.4. Adding these data to the pool of "actual" decadal information ultimately produces ^{14}C ages with a smaller σ.

DECADAL *VERSUS* SINGLE-YEAR AGE CALIBRATION

The smaller INTCAL98 σ comes at a price, of course, because ^{14}C dates of single years and decadal averages need not be identical. The impact on the decadal averages can be assessed by comparing single-year ^{14}C ages (Stuiver, Reimer and Braziunas 1998: Table 2) to decadal ones.

Part of single-year $\Delta^{14}C$ (expressed as the per mil (‰) deviation of tree-ring ^{14}C activity from NBS oxalic acid activity, corrected for isotope fractionation, Stuiver and Polach 1977) is tied to 11-yr-cycle solar modulation of atmospheric ^{14}C production. Pacific Northwest single-year data (when averaged with those of a Kodiak Island tree) yield a three-year moving average for the AD 1897–1945 interval with 11-yr-cycle $\Delta^{14}C$ modulation averaging 2.5‰ (peak to peak) over four cycles (Stuiver and Braziunas 1998). Twenty ^{14}C years appears to be an upper limit for single-yr ^{14}C age change induced by the 11-yr cycle. The standard deviation introduced by 11-yr modulation around the long-term (*e.g.*, decadal average) trend is a much smaller 8 ^{14}C yr (as derived from a 2.5‰ peak-to-peak sinusoidal $\Delta^{14}C$ cycle).

A frequency distribution of single-year (AD 1510–1950) ^{14}C age differences around a smoothing spline (the spline closely resembles a 10-yr moving average) agrees with a Gaussian scatter σ_2 of 14.4 ^{14}C yr (Fig. 1). The laboratory errors reported with the data predict an average measurement standard deviation σ_1 of 13.4 ^{14}C yr for these ^{14}C age differences. If the additional variability σ_n is attributed to natural causes (*e.g.*, the 11-yr cycle) then, since $\sigma_2^2 = \sigma_1^2 + \sigma_n^2$, the increase in sigma from 13.4 to 14.4 ^{14}C yr would be accounted for by $\sigma_n = 5$ ^{14}C yr. The same technique, when applied to a three-year (instead of single-year) moving average, again produces natural ^{14}C variance with $\sigma_n = 5$ ^{14}C yr ($\sigma_1 = 8.4$ ^{14}C yr and $\sigma_2 = 10$ ^{14}C yr).

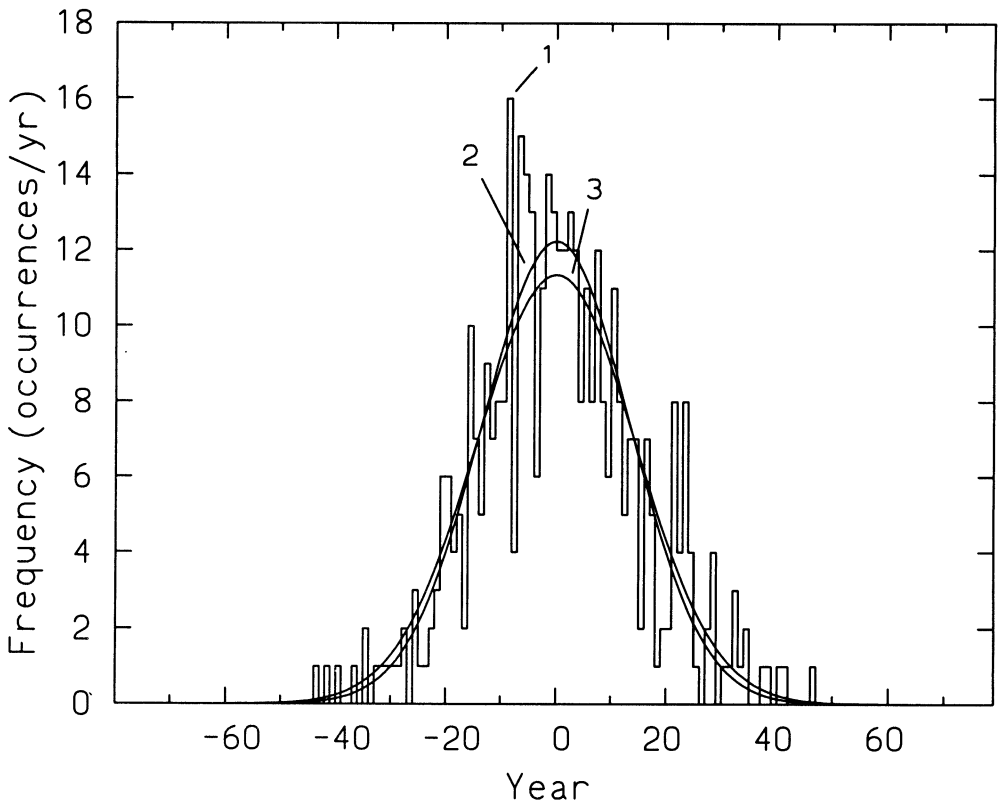

Fig. 1. Plots of the actual frequency distribution of single-year ^{14}C age differences from smoothed spline fitted to a 10-year moving average (AD 1510–1950, diagram indicated by 1), the Gaussian distribution with scatter $\sigma = 14.4$ yr (curve 3), and the Gaussian distribution constructed from the average measurement standard deviation with $\sigma = 13.4$ ^{14}C yr (curve 2)

The above calculations suggest single-year and three-year natural variability (around long-term decadal trends) with σ's in the 5 to 8 ^{14}C yr range (the frequency distribution and solar considerations are for different time intervals). Natural variability plays a role in constructing INTCAL98 "decades" from a mixture of decadal and single (or multiple) year results. Given the above considerations, most INTCAL98 decades should deviate, on average, by only a couple of ^{14}C years from "pure" decadal ones. This statement, of course, only applies to INTCAL98 decades constructed from multiple measurements. When constructing a (hypothetical) INTCAL 98 decade from only one nondecadal ^{14}C age, the INTCAL 98 decadal value would contain, relative to actual decadal values, an additional σ_n in the 5 to 8 ^{14}C yr range.

Information contained in single-year (and three-year) results will be lost to the tune of 5 to 8 ^{14}C yr (σ's) when constructing decadal data. Conversely, when calibrating single-year results against the decadal INTCAL98 curve, the single-year ^{14}C ages will differ from decadal ^{14}C ages (σ in the 5 to 8 ^{14}C yr range). Here we recommend, prior to calibration, an increase of sample standard deviation σ_x to $\sqrt{(\sigma_x^2 + 8^2)}$. The correction is very minor for most samples and only plays a role in high-precision determinations (a σ_x of, *e.g.*, 10 ^{14}C yr transforms into 13 ^{14}C yr).

https://doi.org/10.1017/S0033822200019123 Published online by Cambridge University Press

TREE-RING ^{14}C AGE OFFSETS, "ERROR MULTIPLIERS" AND MINOR ADJUSTMENTS

The major laboratories involved in the determination of tree-ring ^{14}C for INTCAL98 purposes are Seattle (S), Belfast (B), Heidelberg (H), and Pretoria/Groningen (P/G). For the tree-ring cal age portion of the INTCAL98 calibration curve we used the data sets reported in this calibration issue (Stuiver, Reimer and Braziunas 1998; Kromer and Spurk 1998; and McCormac *et al.* 1998a), and previously reported ^{14}C sequences (Vogel and van der Plicht 1993; Pearson, Becker and Qua 1993; Kromer *et al.* 1986; McCormac *et al.* 1998b). When applicable, the older German oak and pine chronologies were adjusted in conformity with the Spurk *et al.* (1998) corrections.

The ^{14}C age differences of samples of identical cal age yield an average offset and (scatter) standard deviation σ_2. The σ_2 can be compared to the standard deviation (σ_1) predicted for the ^{14}C age differences from the laboratory reported errors. The increase in variance (excess variance) σ_E is derived from $\sigma_E^2 = \sigma_2^2 - \sigma_1^2$, whereas the ratio σ_2/σ_1 yields the "error multiplier" k (Stuiver 1982).

The above statistical considerations are valid for ^{14}C determinations of identical samples. However, the samples to be compared here are rarely fully identical, because the time over which the sample was formed may differ (*e.g.,* 10 yr *vs.* 3 yr). Furthermore, cal ages (time-midpoints) of the wood used by different laboratories samples differ. Different selection criteria (*e.g.,* should two samples be compared if one is a 10-yr and the other a 3-yr sample, and the difference in midpoints is ten years) yield variations in σ_E (and k) estimates. Given these uncertainties, the σ_E and k calculations are only approximate.

The interlaboratory comparisons provide information on the sum total of uncertainty tied to the processes of wood allocation, dendroage determination, sample pretreatment, laboratory ^{14}C determination, regional ^{14}C differences and individual tree ^{14}C differences.

^{14}C results determined in different laboratories for samples of the "same" dendroage usually yield offsets in the 0–20 ^{14}C yr range. Values twice as large are occasionally encountered. The larger offsets are, for reasons unknown, over shorter (century-scale) intervals.

Offset information can be derived from ^{14}C age comparisons when results are available from three or more laboratories over an identical time interval. Because average S ^{14}C ages between 6600 and 5800 cal BC differed more than 2σ from those reported by H and B, we increased the S ^{14}C ages over this interval by 27 ^{14}C yr for INTCAL98 purposes. The offset correction is relatively mild: we allow a 2σ difference between the corrected S average and the average of the other laboratories. The same technique reduces Heidelberg ^{14}C ages by 31, 27, and 26 yr for, respectively, 4400–4200, 5200–5000, and 7200–7000 cal BC. The ^{14}C age offsets (number of comparisons = n) between the individual laboratory data sets used for INTCAL98 construction (the minor corrections discussed above are included), as well as σ_1, σ_E, and k, are listed in Table 1.

The trees forming the dendrodated portion of the INTCAL98 curve are predominantly from South Germany, Ireland, California and Washington. For the data sets used for INTCAL98 construction we list in Table 2 tree species, regions, offsets, σ_1, σ_E and k (relative to Seattle). The offsets need not be specifically species-related, and ^{14}C results for trees from different regions may reflect laboratory, as well as regional, influences.

Time-dependent millennium offsets, relative to the INTCAL98 curve, are listed in Table 3. The largest millennium offset of 26 ^{14}C yr, based on a small number of points, is not very significant given the ±10 ^{14}C yr standard deviation. The complete data sets of individual laboratories differ only marginally (up to 11 ^{14}C yr) from INTCAL98.

TABLE 1. A comparison of Seattle, Belfast, Pretoria/Groningen (P/G) and Heidelberg ^{14}C ages of dendrodated wood. The offset equals the weighted mean ^{14}C age difference of samples for which the midpoint cal ages fall within the same decade. n is the number of comparisons, σ_1 is the predicted average standard deviation in single ^{14}C age comparisons (based on quoted laboratory errors), σ_E represents the difference between the observed standard deviation in the age difference (σ_2) and σ_1 (see text). The σ_2/σ_1 ratio = k. Offset, σ_1 and σ_E are in ^{14}C yr.

Laboratories	Offset	σ_1	s_E	k	n	Cal yr interval
Belfast – Seattle	12 ± 1	27	22	1.29	866	7745 BC–AD 1935
Heidelberg – Seattle	19 ± 2	40	22	1.14	230	9665–4085 BC
P/G – Seattle	17 ± 1	22	17	1.26	194	3905–1935 BC
Heidelberg – Belfast	30 ± 3	43	30	1.22	142	7715–4075 BC
P/G – Belfast	−2 ± 2	26	23	1.33	194	3905–1935 BC

TABLE 2. A comparison of tree-ring ^{14}C results of laboratories involved in the INTCAL98 project. (See Table 1 for nomenclature.) Offset, σ_1 and σ_E are in ^{14}C yr.

Laboratories	Offset	σ_1	s_E	k	N	Cal yr interval
Belfast – Seattle Irish oak – U.S. conifers	14 ± 2	24	11	1.1	202	150 BC–AD 1940
Belfast – Seattle Irish oak – German oak	11 ± 1	26	22	1.3	501	5210 BC–AD 30
P/G – Seattle both German oak	17 ± 2	22	17	1.3	194	3910–1930 BC
Belfast – Seattle both German oak	10 ± 2	32	35	1.5	181	7750–5260 BC
Heidelberg – Seattle both German oak	21 ± 3	41	28	1.2	128	7720–4080 BC
Heidelberg – Seattle both German pine	16 ± 4	38	12	1.0	102	9670–8000 BC

A portion of the variance increase (expressed by σ_E or k) is tied to factors unrelated to the laboratory operation (*e.g.*, variable regional ^{14}C differences). Previously (in 1993) k = 1.6 was used to calculate the errors in the decadal Seattle ^{14}C age calibration curve. The Table 1 data suggest k values of 1.14 to 1.33. A conservative k = 1.3 was chosen for the calculation of the errors in decadal INTCAL98 tree-ring ^{14}C ages.

HEMISPHERIC AND REGIONAL OFFSETS

Latitude-dependent differences in ocean surface area, and ocean circulation, cause corresponding latitude-dependent ^{14}C transfer to and from the oceans. Rapid tropospheric mixing of air masses counteracts the oceanic influence but does not fully nullify the atmospheric response. As suggested by an atmospheric transport model (GISS GCM), regional atmospheric $\Delta^{14}C$ gradients may amount to several per mil, especially between Northern and Southern Hemispheric localities (Braziunas, Fung and Stuiver 1995).

The INTCAL98 tree-ring data set is based on a mix of mid-latitude Northern Hemisphere trees (Germany, Ireland, Washington, Oregon and California). The atmospheric transport model predicts $\Delta^{14}C$

https://doi.org/10.1017/S0033822200019123 Published online by Cambridge University Press

TABLE 3. Offsets (millennial time separation) between individual laboratory and INTCAL98 (I) results. P/G is Pretoria/Groningen. All parameters following the cal age interval are in ^{14}C yr. (See Table 1 for nomenclature.)

	I – Seattle		I – Heidelberg		I – Belfast		I – P/G	
Cal age interval	Offset	σ_1	Offset	σ_1	Offset	σ_1	Offset	σ_1
10 – 9 ka BC	3 ± 4	29	−4 ± 5	36				
9 – 8 ka BC	7 ± 3	28	−7 ± 4	33				
8 – 7 ka BC	0 ± 3	28	−12 ± 5	39	11 ± 4	31		
7 – 6 ka BC	2 ± 2	23	−11 ± 5	41	−1 ± 3	29		
6 – 5 ka BC	9 ± 2	23	−26 ± 10	40	−16 ± 3	26		
5 – 4 ka BC	7 ± 2	21	−19 ± 4	34	0 ± 3	27		
4 – 3 ka BC	10 ± 2	17			−8 ± 2	24	−5 ± 2	16
3 – 2 ka BC	9 ± 2	18			−6 ± 2	21	−7 ± 2	19
2 – 1 ka BC	0 ± 2	20			0 ± 2	24	3 ± 6	18
1 – 0 ka BC	2 ± 2	18			−4 ± 2	23		
AD 0 – 1 ka	3 ± 2	18			−9 ± 3	26		
AD 1 – 2 ka	1 ± 1	11			−13 ± 2	19		
10 ka BC – AD 2 ka	**3 ± 1**	**21**	**−11 ± 2**	**37**	**−6 ± 1**	**25**	**−6 ± 1**	**18**

differences of ~1‰ for these areas. Such differences are at the limit of ^{14}C dating and difficult to measure. The fine structure in ocean circulation (*e.g.,* in coastal waters) and differences in regional carbon cycle sources and sinks (*e.g.,* permafrost areas, Damon *et al.* 1996) increase Northern Hemispheric $\Delta^{14}C$ variability. The location-dependent $\Delta^{14}C$ offsets also need not be constant over time. Measurements (not necessarily covering identical time intervals but mostly of the 19th century) of Northern Hemispheric localities yield differences (relative to Washington) of *ca.* −21, *ca.* +22, 16 ± 9, −26 ± 6 (AD 1545–1615), 2 ± 6 (AD 1615–1715), and 14 ± 3 ^{14}C yr for, respectively, the Santa Catalina Mountains in Arizona (Damon 1995), Mackenzie River Valley, Canada (Damon 1995), Dean of Forest oak, England (Stuiver and Quay 1981), Russia (high latitude, two comparisons) and Kodiak Island, Alaska (Stuiver and Braziunas 1998). Furthermore, Irish oak yielded 41 ± 9 ^{14}C yr younger dates than bristlecone pine of Nevada (McCormac *et al.* 1995) and German oak was 23 ± 6 ^{14}C yr younger than California sequoia (Stuiver 1982).

Southern Hemisphere offset measurements (Stuiver and Braziunas 1998) yield 25 ± 7 ^{14}C yr for Tasmania–Washington (19th century), and 38 ± 5 ^{14}C yr and 21 ± 5 ^{14}C yr for South Chile–Washington (respectively, AD 1670–1722 and 19th century). Other offsets are 40 ± 5 ^{14}C yr for South Africa–the Netherlands (AD 1835–1900, Vogel *et al.* 1993) and 27 ± 5 ^{14}C yr for New Zealand–British Isles (AD 1720–1885, McCormac *et al.* 1998a).

For the 1993 calibration program (Stuiver and Reimer 1993), a 40 ^{14}C yr correction was recommended for the entire Southern Hemisphere. The recent measurements of 19th century wood (Tasmania, New Zealand, South Chile) are in line with a smaller Southern Hemispheric offset of 24 ± 3 ^{14}C yr.

The above Southern Hemisphere–Washington offset is for "natural" conditions. During the first half of the 20th century, fossil fuel CO_2 release depressed atmospheric ^{14}C levels to a greater extent in the Northern Hemisphere. Whereas 19th century Chile/Tasmania ^{14}C ages are about 23 yr older than those of Washington, the offset is reduced during the first half of the 20th century. There is even a switch to younger Southern Hemispheric ages *ca.* AD 1940 (Stuiver and Braziunas 1998; McCormac *et al.* 1998b).

https://doi.org/10.1017/S0033822200019123 Published online by Cambridge University Press

TREE-RING AND CORAL ^{14}C AGE DIFFERENCES

The ^{14}C ages of dendrodated tree-rings, together with $^{230}Th/^{234}U$-dated corals, ultimately yield the ^{14}C age axis of the INTCAL98 curve. Tree-cellulose ^{14}C activity reflects the atmospheric $^{14}C/^{12}C$ ratio of CO_2, after correction for isotope fractionation. Similarly, coral-carbonate ^{14}C activity mirrors the mixed ocean layer $^{14}C/^{12}C$ ratio. The ^{14}C-specific activity in the mixed layer (depth ~75 m) is lower than that in the atmosphere because mixed-layer ^{14}C depends on atmospheric as well as deep ocean ^{14}C supply (the main cause for the lower ^{14}C activity of the deep ocean is radioactive decay during its ~1000 yr isolation from the atmosphere). Because ^{14}C ages are based on comparison to a (postulated) stable atmospheric ^{14}C level (*via* the oxalic acid standard), the coral ^{14}C dates have to be corrected for mixed layer ^{14}C reservoir (R) ages.

Late Holocene (preanthropogenic) ^{14}C reservoir ages in the Atlantic, Pacific and Indian Oceans depend on geographic latitude. As luck has it, the tropical areas where coral reefs are formed are part of the oceanic 40°S–40°N region with a fairly constant (non-latitude dependent) pre-bomb R of 300 to 500 ^{14}C yr (Bard *et al.* 1994; Bard 1988; Edwards *et al.* 1993; Burr *et al.* 1998 with 35 pre-bomb samples yielding 494 ± 10 yr for Vanuatu).

R is the ^{14}C age difference between samples grown in equilibrium with the atmosphere, and the mixed layer of the ocean. To make tree-ring and coral results from the 19th century compatible, coral ^{14}C dates should be reduced by 300 to 500 ^{14}C yr. A similar correction does not automatically apply to older samples because ocean and climate variables (rates of deepwater formation and upwelling, average wind speed, ice cover, *etc.*) influence R values (Bard *et al.* 1994).

Tropical paleo-R values of the Early Holocene can be estimated from tree-ring (INTCAL98 values) and coral ^{14}C age differences. Estimated errors used for the following ^{14}C age difference calculations are 2σ for coral ages, and 1σ for INTCAL98 tree-ring ages.

For the 11,800–8300 cal BP interval, the Bard *et al.* (1998), Burr *et al.* (1998), and Edwards *et al.* (1993) coral data yield tree-ring–coral offsets of, respectively, 298 ± 33 ^{14}C yr (11,590–8450 cal BP, number of comparisons n = 19), 537 ± 38 ^{14}C yr (11,770–11730 cal BP, n = 5) and 587 ± 29 (11,045–8363 cal BP, n = 10). Omitting one outlier from the Edwards *et al.* data reduces the 587 ± 29 ^{14}C yr to 502 ± 33 ^{14}C yr. Without the outlier, the weighted average offset for all samples is 440 ± 21 ^{14}C yr.

Differences between oceans are relatively small: R is 406 ± 65 ^{14}C yr (11,590–8450 cal BP, n = 6) for the Atlantic Ocean and 440 ± 20 ^{14}C yr (11,770–8363 cal BP, n = 27) for the Pacific (one outlier omitted). However, there is the suggestion of substantial Pacific intraocean R difference with R = ~300 ^{14}C yr for Tahiti *vs.* R = ~500 ^{14}C yr for New Guinea and Vanuatu.

Between 10,000–8,000 and 12,000–10,000 cal BP the coral data generate a weighted mean R value of, respectively, 414 ± 31 ^{14}C yr (n = 12) and 509 ± 25 ^{14}C yr (n = 21). Omitting the outlier reduces the latter to R = 451 ± 26 ^{14}C yr. The older sample ages appear to have slightly larger R's, as depicted by the 1000 yr averages in Figure 2. Good agreement between mixed-layer corrected coral dates and tree-ring ^{14}C dates (Fig. 3) is obtained when using R = 500 and 400 ^{14}C yr for, respectively, the 12,000–10,000 cal BP and 10,000–8000 cal BP intervals.

Future adjustments of the pine–oak chronology, if any, will influence the derived R values. The 100 ^{14}C yr R "increase" is perhaps tied to missing rings in the earliest part of the pine tree-ring chronology. Given our current state of knowledge, however, we do accept an R value of 500 ^{14}C yr for the 12,000–10,000 cal BP interval, and postulate the same tropical R for the Late Glacial ocean.

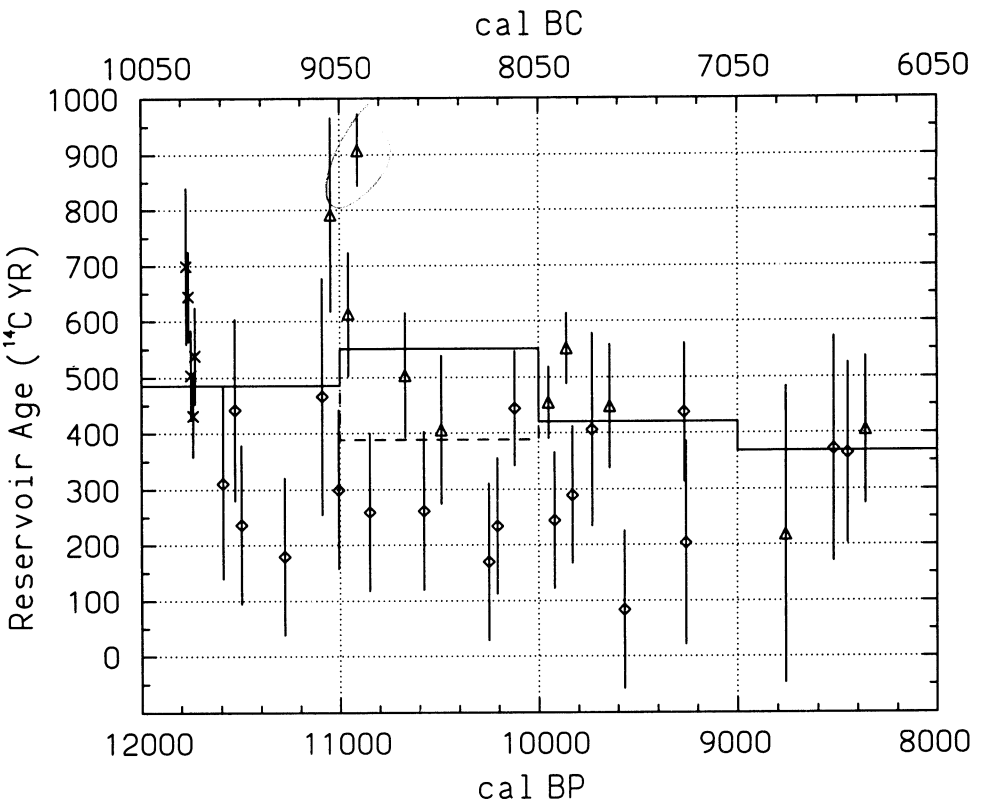

Fig. 2. Reservoir ages (^{14}C age difference between coral and tree-ring samples of similar cal age) between 12,000 and 8000 cal BP. Coral measurements given here and in the following figures are from Bard *et al.* 1998 (◇), Burr *et al.* 1998 (×), Edwards *et al.* 1993 (△). R values averaged over millennia are represented by the solid line. The dashed line is the R value for the 11,000–10,000 cal BP millennium when omitting the 900 ^{14}C yr data point. Vertical bars represent the calculated error in the ^{14}C age difference calculation, based on a 2σ error in the coral ^{14}C age determination, and a 1.3σ error in the tree-ring ^{14}C age determination.

CORAL ^{14}C AGE VARIABILITY

The corals are assumed to be ideal closed systems with regard to ^{14}C, ^{234}U and ^{234}Th exchange. The overall agreement (Fig. 3) between reservoir-corrected coral (with the reservoir correction averaged over millennia), and tree-ring ^{14}C dates suggests that this condition is fairly well adhered to for carefully collected samples. Nevertheless, the scatter σ_2 of INTCAL98 tree-ring minus reservoir-corrected coral ^{14}C ages (12,000–8000 cal BP, n = 33) is 260 ^{14}C yr, whereas the quoted measuring precision alone produces a σ_1 = 69 ^{14}C yr, resulting in σ_E = 255 ^{14}C yr and error multiplier k = 3.7. Similar comparisons between tree-ring data sets yield an average k value of only ~1.3.

The above calculation uses a fixed R of 500 and 400 yr for, respectively, 12,000–10,000 cal BP and 10,000–8000 cal BP. Normalizing each individual data set on its own R value (which aligns the average of each individual coral data set with that of the INTCAL98 tree-ring record) yields an improved k = 2.3 when the INTCAL98 reservoir-corrected ^{14}C ages are subtracted from the tree-ring ages.

To generate a pre-12,000 cal BP atmospheric record, one has the choice of 1) assuming R to be constant for each individual site, or 2) assuming average tropical R to be constant (the 500 ^{14}C yr dis-

https://doi.org/10.1017/S0033822200019123 Published online by Cambridge University Press

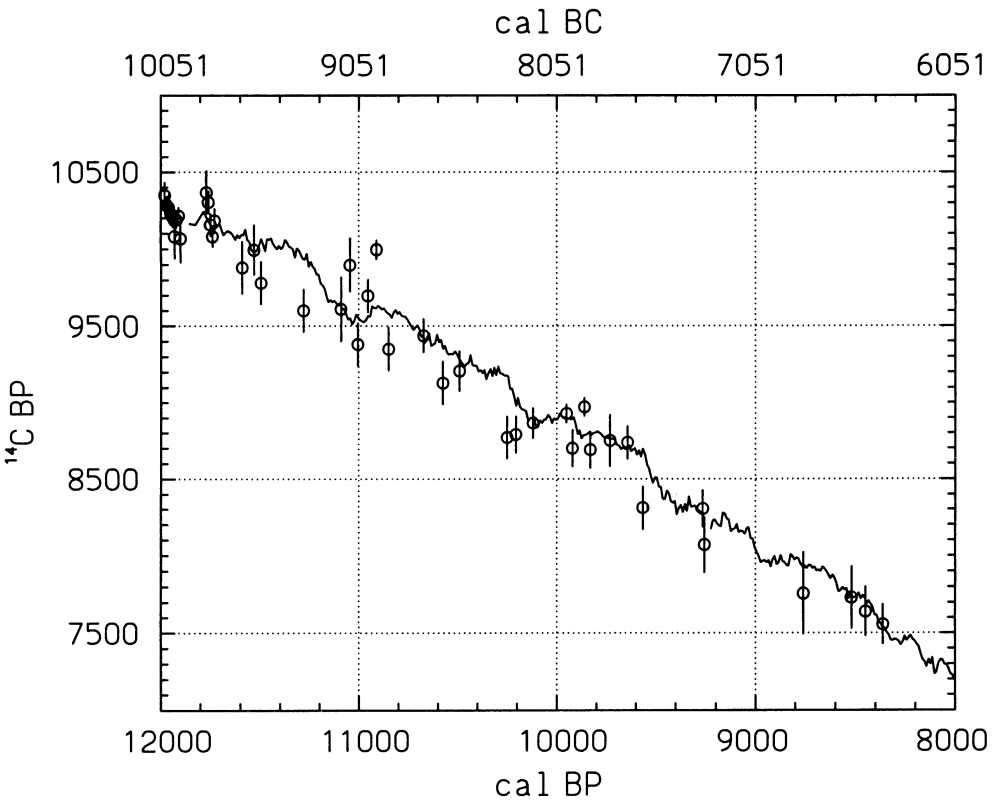

Fig. 3. Position of coral ^{14}C ages (o), relative to INTCAL 98 tree-ring ^{14}C ages (solid line), after a reservoir deficiency correction of the coral ^{14}C ages by 400 and 500 ^{14}C yr for, respectively, 10,000–8000 cal BP and 12,000–10,000 cal BP. Vertical bars equal 2σ in the coral ^{14}C age measurement.

cussed previously). It is likely (but not proven) that prior to 12,000 cal BP single-site R variability was larger than average R variability. We decided to generate the pre-12,000 cal BP atmospheric record by deducting an average tropical R = 500 ^{14}C yr from all coral data.

The atmospheric and mixed-layer ^{14}C records are filtered differently by natural processes. Mixed-layer response to postulated decadal atmospheric forcing resembles a ~100–200 yr moving average (*e.g.*, Stuiver, Reimer and Braziunas 1998). Using a similar 200-yr moving average for tree rings, however, does not reduce the coral ^{14}C–tree-ring σ_E. Mechanisms resulting in increased variance could be 1) varying tropical reservoir deficiency R, 2) post-depositional ^{14}C activity modification and 3) U/Th age uncertainty.

Post-depositional ^{14}C modification can be accounted for by using twice the standard deviation of the measurement. Many investigators routinely double the measuring precision of coral ^{14}C determinations (Edwards *et al.* 1993; Bard *et al.* 1990). For INTCAL98 purposes the assigned standard deviation of coral ^{14}C ages is based on a 2σ error in the coral ^{14}C age determination, and a k = 1.3 error multiplier similar to the one used for tree-ring derived ^{14}C ages. The combined multiplier of 2.6 accounts for most of the variance actually observed.

https://doi.org/10.1017/S0033822200019123 Published online by Cambridge University Press

MARINE RESERVOIR AGE CONSIDERATIONS

Causes for century-scale atmospheric ^{14}C variability include solar modulation of the cosmic-ray flux and ocean circulation change. Model calculated R values depend on the forcing mechanism. Switching from a solar to an oceanic mode produced century-scale global R change of ~150 ^{14}C yr in a global carbon reservoir model (Stuiver, Reimer and Braziunas 1998).

Splining of the reservoir-corrected coral ^{14}C ages (R = 500 ^{14}C yr) generates the pre-11,850 cal BP portion of the "atmospheric" INTCAL98 calibration curve. Before 11,850 cal BP, tropical ocean R is assumed to be identical for the Atlantic, Pacific and Indian Ocean, as well as nonvariable over time. It is difficult to estimate the limits of tropical R change. Figure 2 suggests tropical R change of only ~100 ^{14}C yr for millennia-scale oceanic changes between the end of the Ice Age and 8000 cal BP. A comparison of Cariaco Basin (Hughen *et al.* 1998) varve and INTCAL98 tree-ring chronologies (discussed in the following section) suggests that decadal- to century-scale tropical R variability is restricted to ~100 ^{14}C yr (11,700–9000 cal BP interval). Larger millennia-scale tropical R changes further back in time cannot be excluded, but are not very likely given the limited tropical R variability between the end of the Pleistocene and the present.

The globally integrated atmospheric ^{14}C levels, and global R, depend on a globally integrated ocean circulation and ocean-atmospheric exchange rate. To derive global INTCAL98 atmospheric values, we used a constant late-glacial tropical R value of 500 ^{14}C yr. Implied in the switch from tropical to global conditions is the notion that tropical R and global R parallel each other over the 24,000–11,850 cal BP interval.

The corals discussed so far were formed in the mixed surface layer of the tropical ocean. Deep-sea corals, on the other hand, live mostly between 500 and 2000 m depth and are not confined to tropical latitudes. These corals exhibit substantial century-scale deepwater R change in the Atlantic (16,000–12,000 cal BP interval: Adkins *et al.* 1998; Mangini *et al.* 1998). Atlantic deepwater ^{14}C levels are tied to specific deepwater masses (*e.g.,* Stuiver and Östlund 1980) and the deepwater R changes are most likely caused by shifts in their depths. These relatively fast regional ocean circulation changes have the potential to modify (to an unknown extent) the values of both late-glacial atmospheric ^{14}C and mixed-layer R.

MARINE VARVE CHRONOLOGY

Marine sediments of the Cariaco Basin in the Atlantic Ocean (at the northern continental margin of Venezuela) yield a ^{14}C–varve count sequence (Hughen *et al.* 1998) useful for INTCAL98 construction. The floating chronology is tied to the absolute time scale by matching marine ^{14}C ages to the INTCAL98 tree-ring data (the tree-ring data are increased by 500 and 400 ^{14}C yr for, respectively, 12–10 and 10–8 ka cal BP). The best fit between the ^{14}C ages of the adjusted tree-ring record and the Cariaco Basin is shown in Figure 4. The absolute time scale produced in this manner for the floating varves reduces the Hughen *et al.* (1998) varve count time scale by 40 yr. The latest tree-ring and R adjustments cause this minor difference. The matching is secure within a statistical error (one σ) of 15 yr.

Applying R = 400 (10–8 ka cal BP) and 500 (14.5–10 ka cal BP) ^{14}C yr to the corals and calibrated varve series yields the Figure 5 "atmospheric" values. Relative to the INTCAL 98 tree-ring record, the varve-derived ^{14}C ages scatter less (k = 1.3) than the coral ^{14}C ages. The observed varve scatter σ of ~95 ^{14}C yr (11,700–9000 cal BP interval) suggests a ~100 ^{14}C yr limit on tropical R change on decadal/century time-scales.

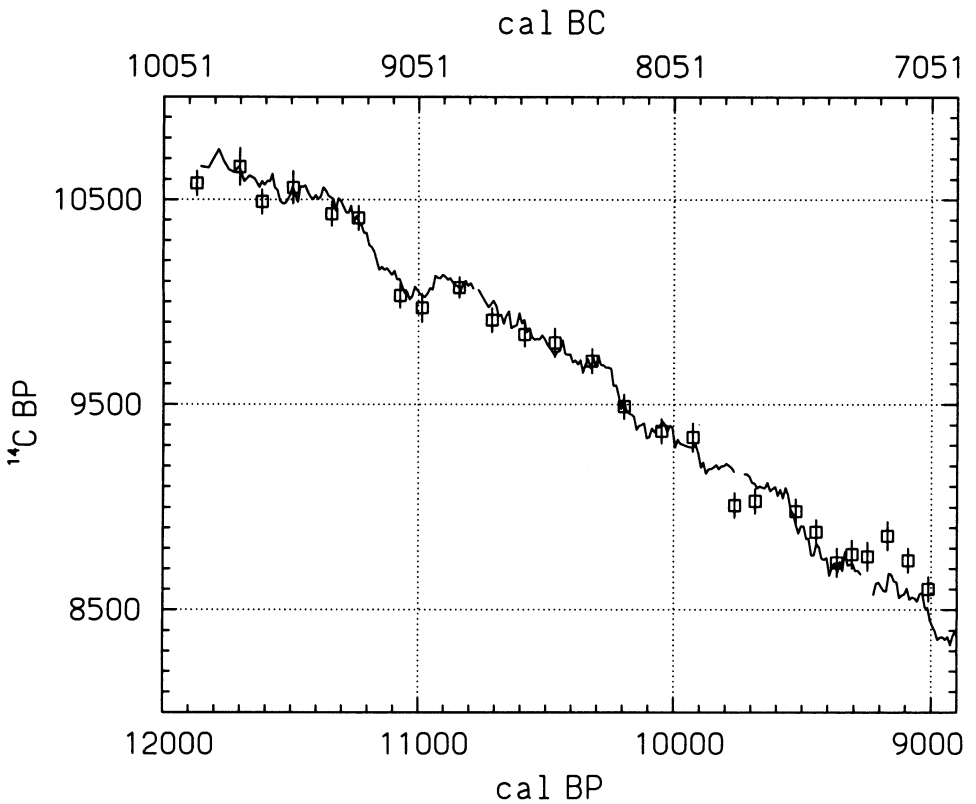

Fig. 4. Cal BP calibration of a floating marine varve record. The varve data given here, and in the following figures, are from Hughen *et al.* (1998). Shown is the best fit between the marine equivalent of the INTCAL98 tree-ring record (solid line, R values as noted with Fig. 3 were applied) and the measured varve results (□, with 1σ bars).

ATMOSPHERIC AND MARINE INTCAL98 CONSTRUCTION

The atmospheric INTCAL 98 curve consists of two segments, each derived from diverse materials and techniques. The materials used are wood (tree rings), coral and marine sediment. The ^{14}C activity measurement is common to all but the cal BP time scale determination differs. The wood samples (back to 11,850 cal BP) are dated through dendrochronological means, the corals through U-Th determinations, and the marine sediment through ^{14}C matching of (floating) varve and tree-ring chronologies. Marine coral and varve data, normalized on atmospheric levels, yield a 24,000–11,850 cal BP extension of the directly measured atmospheric values. Only two coral measurements are available for the 40,000–24,000 cal yr interval, resulting in rather speculative age "calibration" over this interval.

The 11,850–0 cal BP segment was constructed from ^{14}C age measurements reported by the Belfast, Heidelberg, Pretoria/Groningen and Seattle laboratories (Stuiver, Reimer and Braziunas 1998; Kromer and Spurk 1998; McCormac *et al.* 1998a and b; Pearson, Becker and Qua 1993; Vogel and van der Plicht 1993; Kromer *et al.* 1986). Decadal ^{14}C ages back to 11,614 cal BP were constructed by taking the average ^{14}C age of all samples with cal midpoints within the cal decade. The rationale for this approach can be found in the introduction. The 11,624–11,854 cal BP interval is covered by the measurements of a single laboratory (Heidelberg; Kromer and Spurk 1998) of 20- to 30-yr tree-ring samples. The segments of Figure A8–A19 (Appendix) depict for 1000 cal yr intervals the "dec-

https://doi.org/10.1017/S0033822200019123 Published online by Cambridge University Press

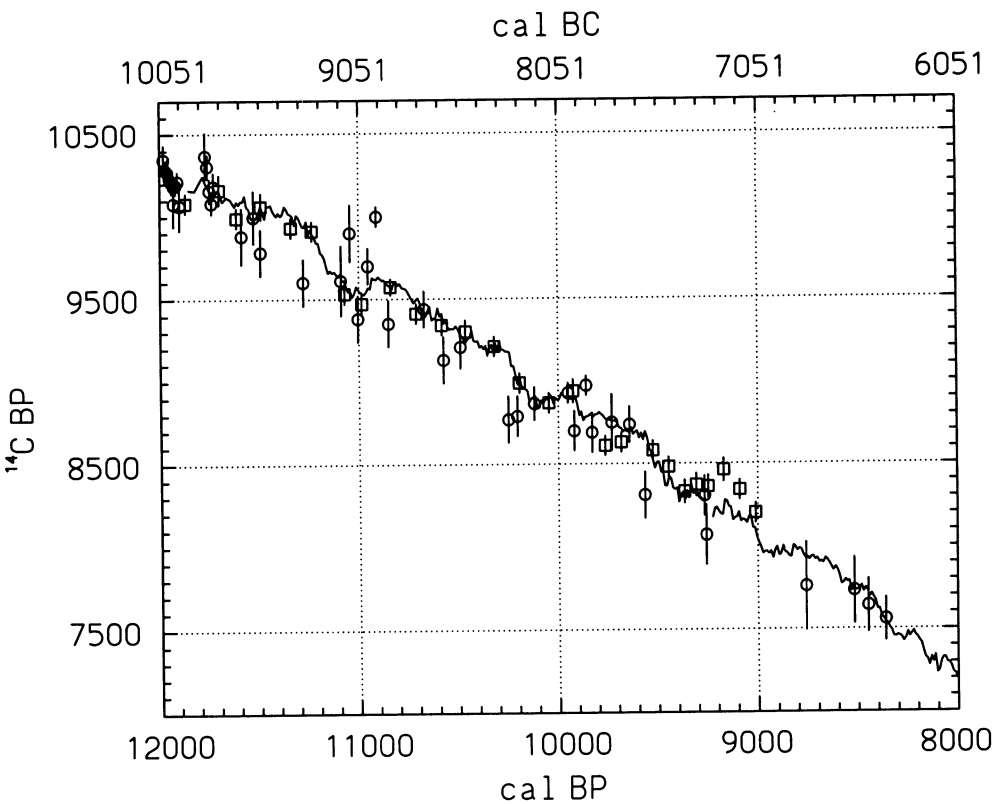

Fig. 5. INTCAL 98 tree-ring ^{14}C ages (solid line) and the atmospheric equivalent (obtained by using the R values noted with Fig. 3) of 1) coral ^{14}C ages (O, bar = 2σ) and 2) marine varve ages (□, bar = 1σ). The cal BP ages of the corals were determined by U/Th dating and the cal BP ages of the varves by a floating varve count that was shifted to the position given in Fig. 4.

adal" tree-ring derived portion of the atmospheric INTCAL 98 calibration curve (11,854–0 cal BP). The curve was constructed by linearly connecting the ^{14}C ages obtained for the decadal (plus a few bidecadal) cal age intervals. The INTCAL98 standard deviation (width of the calibration curve, not given in Fig. A) resulted from the linear connection of the ±1.3σ age errors.

The primary data of the 24,000–11,850 cal BP segment are coral and varve measurements (Bard *et al.* 1998; Burr *et al.* 1998; Edwards *et al.* 1993; Hughen *et al.* 1998). The ^{14}C ages of the 12,500–11,850, 15,000–12,500, 19,500–15,000, and 24,000–19,500 cal BP intervals, adjusted to atmospheric levels by deducting a reservoir deficiency of 500 ^{14}C yr (the rather minor 25 ^{14}C yr standard deviation was neglected) from the marine ages, are depicted in Figures 6–9 with vertical bars representing 1σ in the varve ^{14}C determinations, and 2σ for the coral ^{14}C determinations. The "atmospheric" ^{14}C ages of the 40,000–15,000 cal BP interval are given in Figure 10. Coral and varve data coverage is excellent for 16,000–11,850 cal BP, less so for 24,000–16,000 cal BP, and marginal for 40,000–24,000 cal BP.

The minimum smoothing spline (Reinsch 1967) of Figures 6–9, anchored at the last tree-ring point at 11,854 cal BP, was used to generate the atmospheric INTCAL98 ^{14}C ages of the 11,850–16,000 cal BP period. Due to the scarcity of coral samples, INTCAL 98 lacks detail between 24,000 and 16,000 cal BP. Here the spline is essentially linear, with cal BP = 1.15 ^{14}C BP + 680.

https://doi.org/10.1017/S0033822200019123 Published online by Cambridge University Press

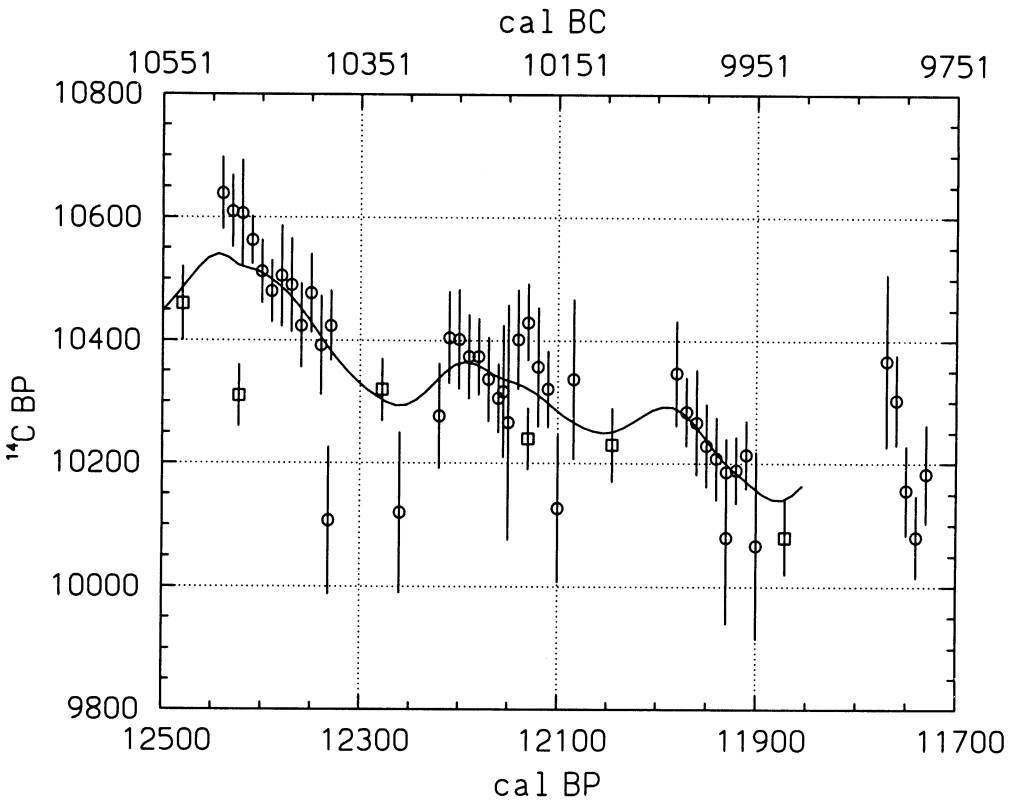

Fig. 6. "Atmospheric" coral (○, bar = 2σ) and varve (□, bar = 1σ) ^{14}C ages. The minimum smoothing spline (solid line), anchored at the last tree-ring point (11,854 cal BP), was used to derive the INTCAL 98 ^{14}C ages of the 12,500–11,854 cal BP time interval.

The 24,000–11,850 cal BP coral- and varve-derived segment of atmospheric INTCAL 98 is part of the Figure A calibration curve. For the marine-derived atmospheric ages we used, as discussed, a spline with minimum smoothing. The INTCAL98 standard deviation (width of the calibration curve) was derived by using a standard deviation of 2σ for the coral ^{14}C ages, 1σ for the varve ^{14}C ages, and a k=1.3 error multiplier for both (σ = standard deviation in the measurement).

There are only two data points between 40,000 and 24,000 cal BP, and a linear relationship is automatic (Fig. 10). This interval, due to the lack of corroborating data points, generates an error-prone calibration curve. The 40,000–24,000 cal BP interval, as a consequence, was not considered for INTCAL98 inclusion.

The conversion of marine ^{14}C age to atmospheric ^{14}C age (by deducting 500 ^{14}C yr from the marine age) is an approximation only. The marine record also contains less detail than the atmospheric one, especially for cosmic-ray induced ^{14}C production rate change (*e.g.*, Stuiver, Reimer and Braziunas 1998). Only the 15,000–12,000 cal BP interval, with a large number of marine data points, produces a century-scale fine structure.

The marine INTCAL98 curve (Fig. B) of the 8800–0 cal BP interval contains marine ^{14}C ages derived from the tree-ring record *via* carbon reservoir modeling (Stuiver, Reimer and Braziunas 1998). Coral and marine varve ^{14}C ages were used for the 24,000–8800 cal BP marine INTCAL98

https://doi.org/10.1017/S0033822200019123 Published online by Cambridge University Press

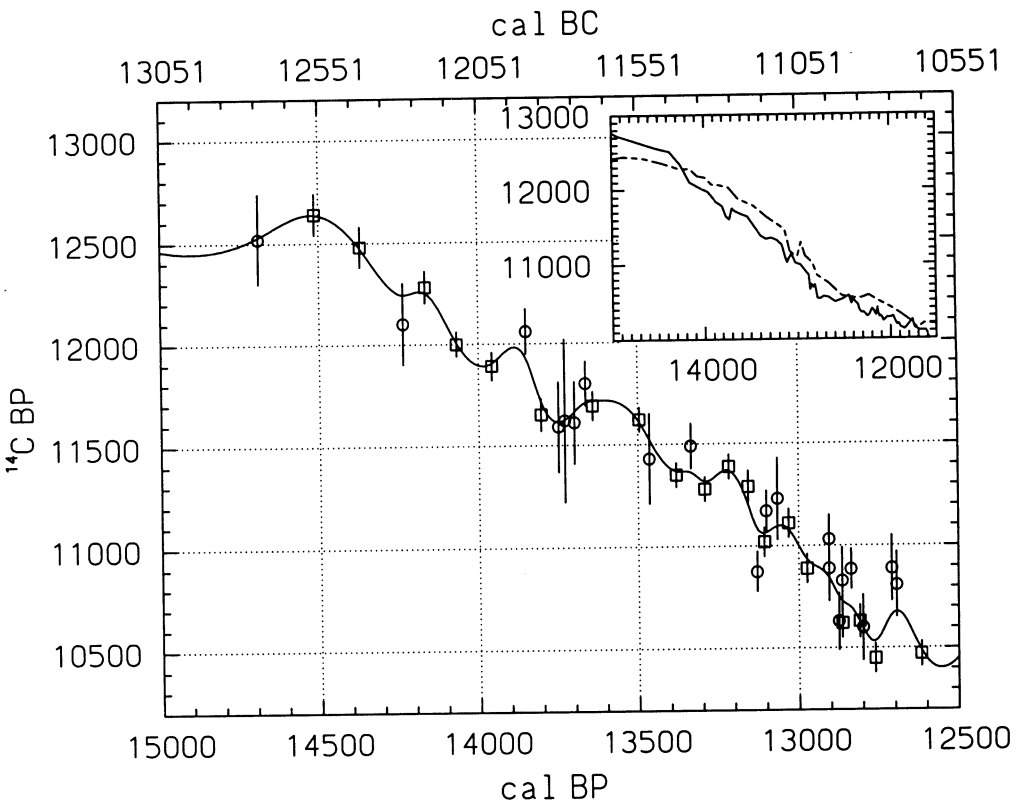

Fig. 7. Splined "atmospheric" coral and varve data 15,000–12,500 cal BP (solid line; see Fig. 6 caption for symbols). The inset compares three-point moving averages of "atmospheric" (marine derived) INTCAL 98 ^{14}C ages (solid line) to a similar moving average of terrestrial ^{14}C ages (dashed line) dated by varves (Kitagawa and van der Plicht 1998).

segment. Here we splined the available marine ^{14}C dates of the 15,585–8800 cal BP interval (Figs. 5–7), and used a linear approximation for the 24,000–15,585 cal BP interval (Figs. 8 and 9). The calculated INTCAL98 standard deviation (width of the calibration curve, not given in Fig. A) was derived from the measured 2σ deviation for the coral ^{14}C ages, 1σ for the varve ^{14}C ages, and a k=1.3 error multiplier for both (σ = standard deviation in the measurement). The connection between the splined and carbon reservoir calculated marine ^{14}C ages is depicted in Figure 11.

The INTCAL98 marine calibration curves (Fig. B) reflect global open ocean conditions. Regional departures from the global values can be expressed in a ΔR parameter, as discussed in Stuiver, Reimer and Braziunas 1998.

INTCAL98 Δ^{14}C

Converting the atmospheric ^{14}C ages into Δ^{14}C values yields Figure 12. The long-term trend in Δ^{14}C is usually attributed to geomagnetically induced ^{14}C production rate change.

An interesting Δ^{14}C comparison can be made with the recently published 45,000 cal BP atmospheric varve chronology (Kitagawa and van der Plicht 1998). Although for the 15,000–12,000 cal BP interval the long-term trends of the Kitagawa and van der Plicht atmospheric record and the INTCAL98 atmospheric record derived from marine data are similar, century-scale detail is less fine in the varve

https://doi.org/10.1017/S0033822200019123 Published online by Cambridge University Press

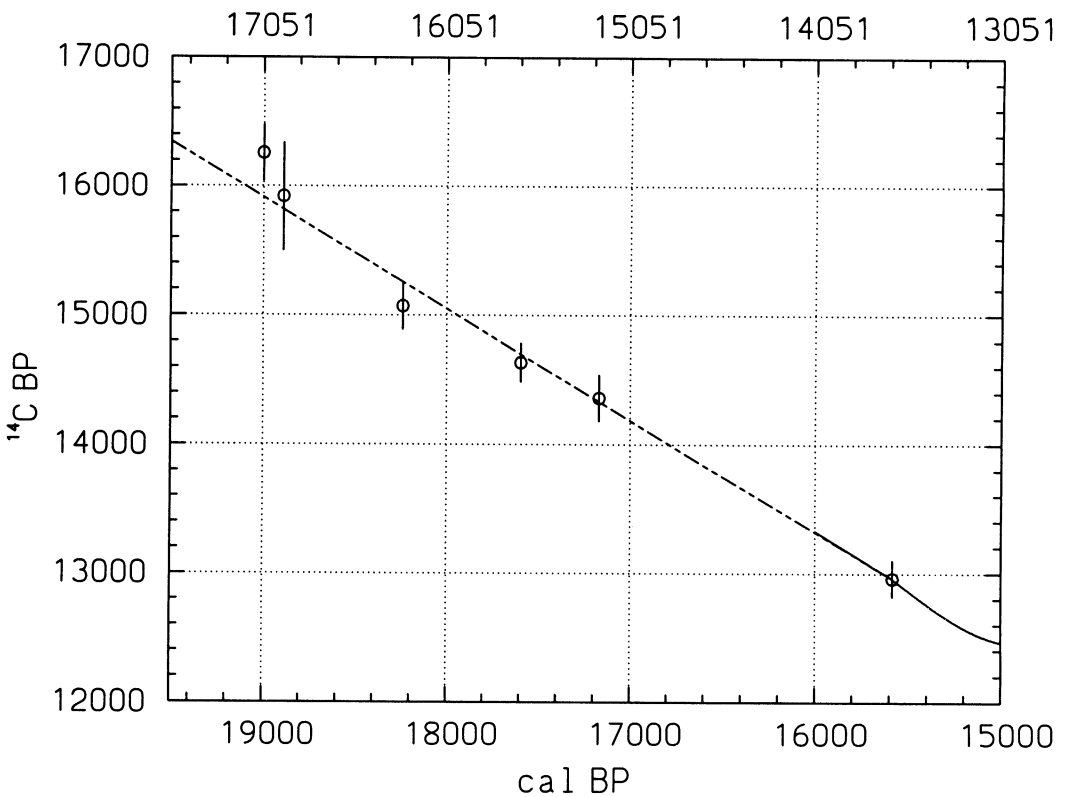

Fig. 8. Splined "atmospheric" coral data (19,500–15,000 cal BP; see Fig. 6 for symbols). The number of data points is too small to generate detail in the dashed curve.

record (the inset in Fig. 7 compares three-point moving averages of both data sets). The varve curve, on the other hand, is more detailed for pre-15,000 cal BP ages where the coral curve (due to the limited number of data points) appears linear.

Given a perfect varve chronology, the 175-yr offset (Fig. 7 inset) would indicate a marine reservoir correction of 325 ^{14}C yr instead of 500 ^{14}C yr. Because a zero-error varve chronology is unlikely, however, this cannot be definitely concluded.

The century- and millennium-scale Δ^{14}C variations (residual Δ^{14}C, in per mil) of Figure 13 were obtained by deducting a 2000 yr moving average.

Reduced North Atlantic deepwater formation is tied to reduced surface-water transport toward the North (the "warm" Gulf stream), causing Northern regions (*e.g.,* Western Europe and Greenland) to become colder. Reduced deepwater formation is also tied to atmospheric ^{14}C increase. Because lower δ^{18}O values[9] accompany reduced atmospheric precipitation temperatures, one expects an inverse relationship between δ^{18}O and Δ^{14}C for oceanic-induced climate perturbations. The relationship (correlation coefficient r = –0.54, Δ^{14}C/δ^{18}O = –20.4) is depicted in Figure 14, where residual INTCAL98 Δ^{14}C (U/Th time scale) is compared to inverted δ^{18}O (ice layer count time scale) of the GISP2 Greenland ice core (Stuiver, Grootes and Braziunas 1995) for the 15,500–10,500 cal BP interval.

[9] δ^{18}O is the per mil deviation of the sample ^{18}O/^{16}O ratio from that of the SMOW standard .

https://doi.org/10.1017/S0033822200019123 Published online by Cambridge University Press

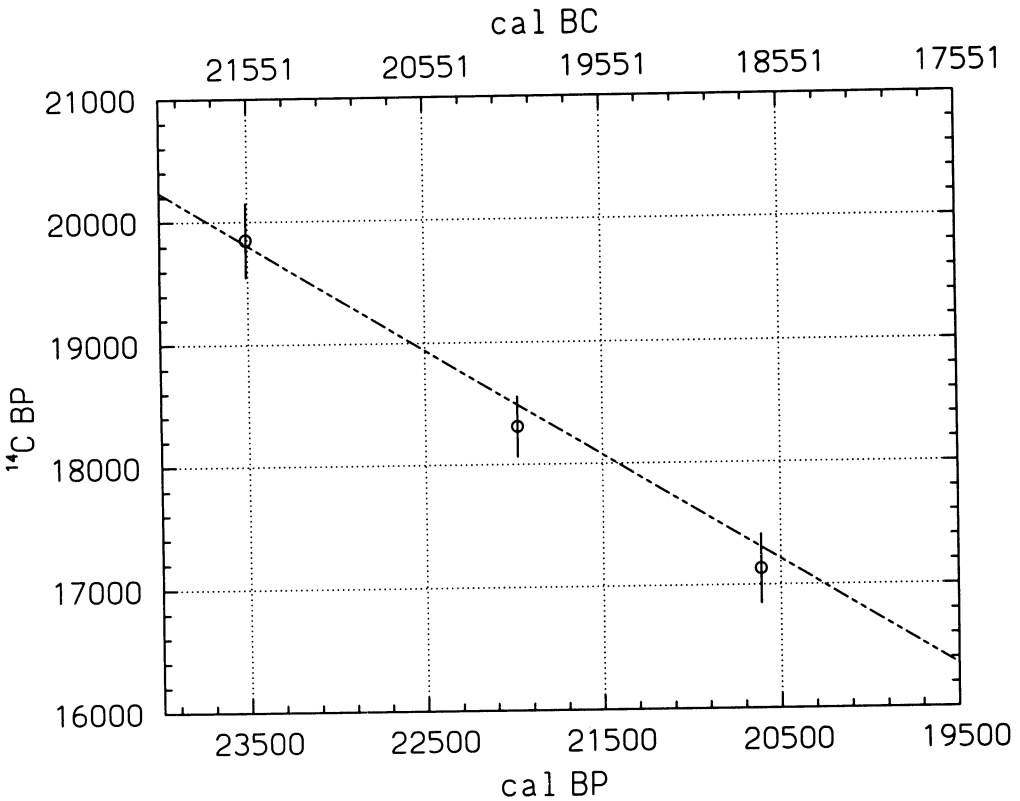

Fig. 9. Splined "atmospheric" coral data (24,000–19,500 cal BP; see Fig. 6 for symbols). The number of data points is too small to generate detail in the dashed curve.

The reduction of residual $\Delta^{14}C$ during the 15,000–14,500 cal BP interval suggests that the temperature increase of the Bølling (which starts *ca.* 14,670 cal BP) is tied to increased deepwater formation. The increase is followed by a two-step reduction and reverses again to increased deepwater formation (Broecker 1997, 1998; Hughen *et al.* 1998; Stuiver and Braziunas 1993) at the beginning of the Younger Dryas (~12,890 cal BP). This increase in deepwater formation ultimately leads to the relatively stable temperatures of the Holocene. To complicate matters, a Younger Dryas bipolar seesaw also may be operating (Broecker 1998). The Holocene itself has several century-scale oceanic and solar-induced (the solar connection yields $\Delta^{14}C = 60\ \delta^{18}O$) $\Delta^{14}C$ perturbations (Stuiver and Braziunas 1993; Stuiver *et al.* 1997).

Oceanic-induced atmospheric $\Delta^{14}C$ changes ($\Delta^{14}C$/yr) are caused by ^{14}C exchange rate variations between the mixed layer and deep ocean. For a complete cessation of ^{14}C transfer between mixed layer and deep ocean, the cosmic-ray-produced ^{14}C (global production rate Q in atoms/yr) will be distributed over a much smaller atmosphere, biosphere and mixed layer (ABM) reservoir. Present-day carbon reservoirs contain ^{14}C totaling 8260 yr of production (8260Q). The ABM reservoir contains only 7% of the total amount of exchangeable carbon (*e.g.*, Lal 1985), or 580 yr of ^{14}C production (580Q). When completely separated from the deep ocean, the atmospheric ^{14}C level of the ABM reservoir will double in *ca.* 650 yr (without radioactive decay the doubling time would be 580 yr). Thus the fastest rate of ^{14}C change in the atmosphere will be ~1% per 7 yr for a hypothetical deep ocean suddenly disconnected from the ABM reservoir. Rates of change of similar magnitude

https://doi.org/10.1017/S0033822200019123 Published online by Cambridge University Press

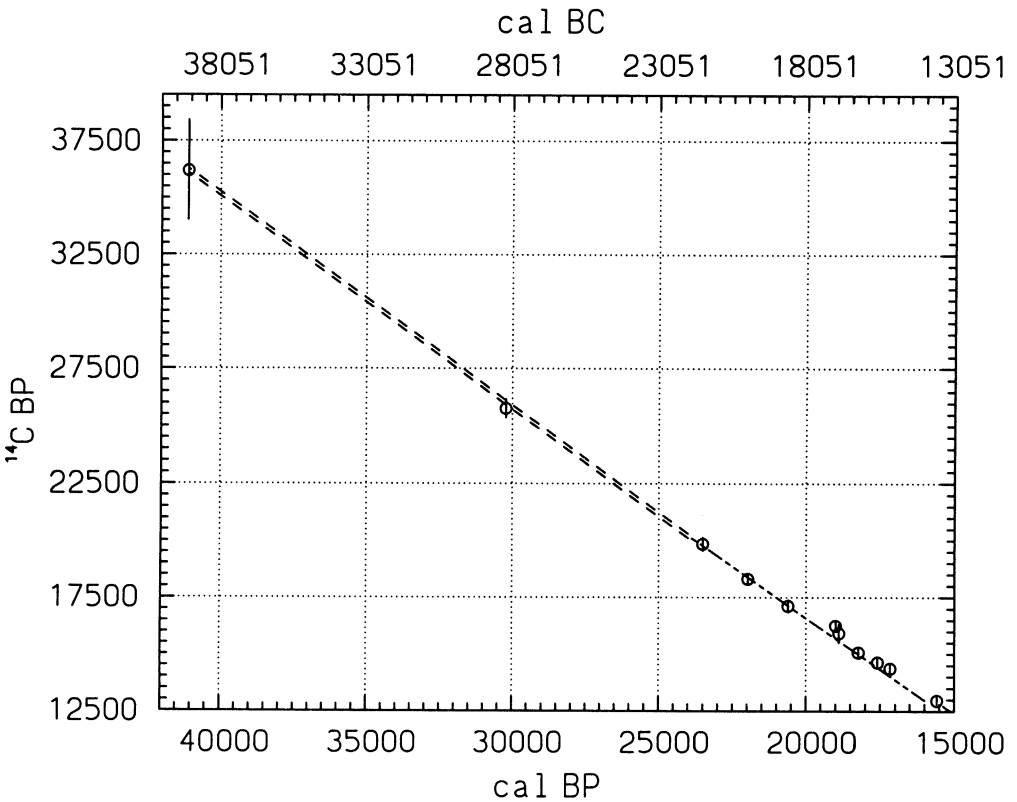

Fig. 10. The extension of the Figs. 6–9 spline to 40,000 cal BP. The double-dashed portion (only two coral measurements) is *not* acceptable as an INTCAL98 calibration curve.

will occur when fully reconnecting the mixed layer and deep ocean (the downward flux (0.93Q) is nearly identical to the production rate Q).

There are two modes of ^{14}C transport from the mixed layer to the deep ocean. Diffusion (including isopycnal advection) and deepwater formation play a key role. For the Holocene, deepwater formation transports about two-thirds of the global ^{14}C to the deep ocean (Toggweiler, Dixon and Bryan 1989). This yields a maximum Δ^{14}C change of 1% per 10.5 yr for full cessation of deepwater formation alone. The fastest observed century-scale Δ^{14}C change of 1% per 17 yr (near 13810, 13140 and 12720 cal BP, Fig. 14) delivers a 60% change in the rate of global deepwater formation. The well-defined maxima and minima in Figure 14 also suggest decadal switching times. And fast switching between the two modes of deepwater formation agrees with the symmetrical shape of several century-scale ^{14}C maxima and minima in Figure 14.

The Δ^{14}C decline near the start of the Bølling produces a fairly long plateau (15,000–14,400 cal BP) in the ^{14}C age–cal age relationship (Fig. 7 and 8). There are several Bølling-type oscillations in the GISP2 oxygen isotope record between 40,000 and 15,000 cal BP. Assuming similarity in atmospheric ^{14}C response, one expects *ca.* 600-yr-long ^{14}C age plateaus near 38,400, 35,300, 33,600, 32,300 and 29,100 cal BP (GISP2 time scale).

https://doi.org/10.1017/S0033822200019123 Published online by Cambridge University Press

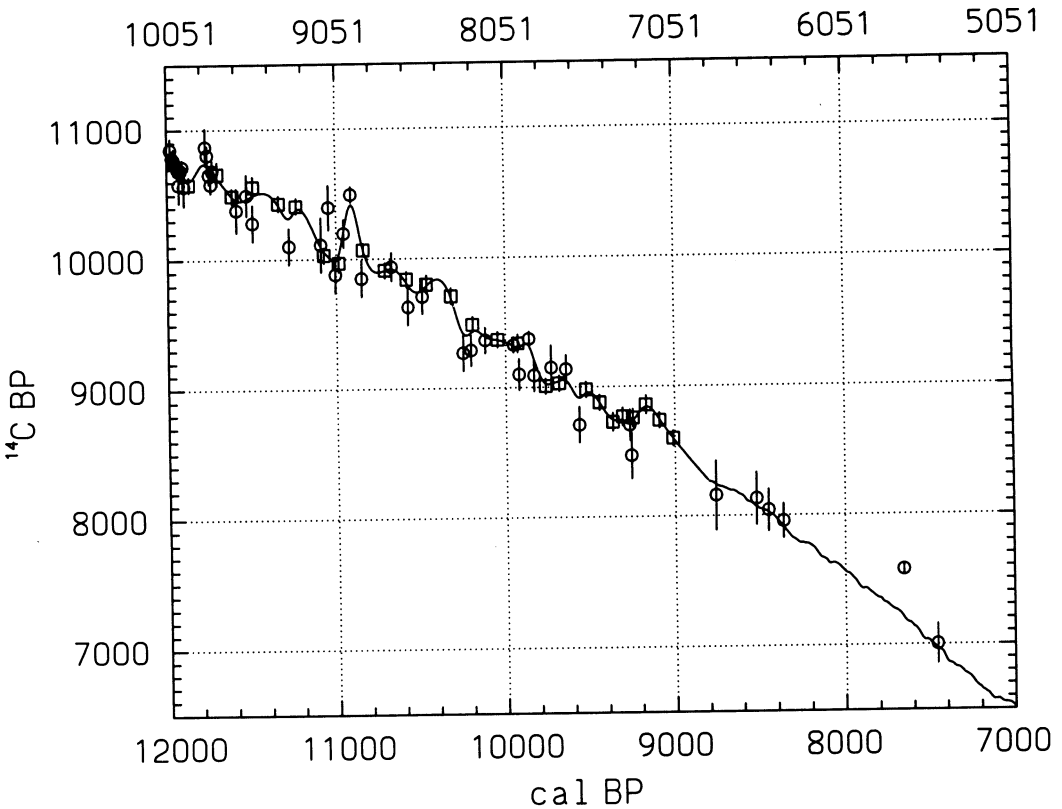

Fig. 11. Coral (○, bar = 2σ) and varve (□, bar = 1σ) ^{14}C ages splined (solid line) over the 12,000–8800 cal BP interval. The spline is connected to the carbon reservoir calculated decadal marine ^{14}C ages (solid line) of the 8800–7000 cal BP interval. The solid lines form the INTCAL98 calibration curve for marine samples.

CALIBRATION

It is not possible to suggest guidelines for specific regional (non-hemispheric) offsets due to the lack of precise information on time-dependent regional ^{14}C differences. Offsets (see "Hemispheric and Regional Offsets") introduce uncertainties of one or two decades in the age calibration process of atmospheric samples. Because the ^{14}C level of the Southern Hemisphere is, on average, below that of the Northern Hemisphere, we recommend for Southern Hemispheric samples a ^{14}C age reduction of 24 ± 3 ^{14}C yr prior to calibration (pre- AD 1900 atmospheric samples only).

As noted previously, the atmospheric calibration curve is based on 1) a linear connection of the tree-ring generated decadal data points (11,850–0 cal BP) and 2) a spline with minimum smoothing of reservoir-corrected coral and varve data (24,000–11,850 cal BP).

The marine calibration curve consists of 1) a linear connection of carbon reservoir calculated decadal marine ages (8800–0 cal BP) and a 2) a spline of measured coral and varve ages (24,000–8800 cal BP) with a degree of smoothing similar to the atmospheric calibration curve.

The standard deviation in the curves is not drawn in Figures A (atmospheric) and B (marine). For the tree-ring based portion of the atmospheric curve, the width of the curve (the one standard deviation includes a 1.3 error multiplier) starts with an average 9 yr for the youngest millennium and increases

https://doi.org/10.1017/S0033822200019123 Published online by Cambridge University Press

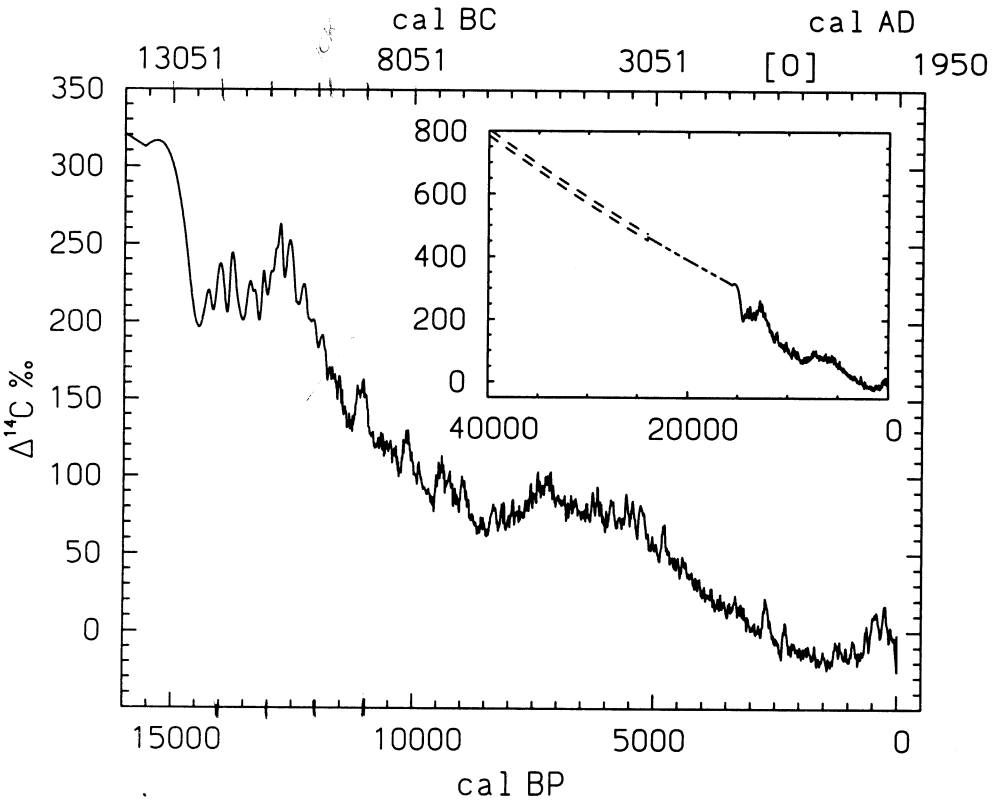

Fig. 12. Atmospheric $\Delta^{14}C$ profile for 1) 15,500–0 cal BP and 2) 40,000–0 cal BP (inset, with $\Delta^{14}C$ per mil scale). Tree-ring data were used for the 11,854–0 cal BP construction and marine (coral and varve) information for the remaining part. The solid line represents $\Delta^{14}C$ values derived from the INTCAL98 ^{14}C age–cal age relationship; the dashed portion is based on the splining of a limited number of data points (see Figs. 7 and 8). The double dashed curve is based on only two measurements.

to 23 yr for the older part (11,000–10,000 cal BP). The width of the spline, derived from the coral and varve ^{14}C age errors, is one standard deviation (as discussed, we use for the calculation of the actual standard deviation 2σ for the coral ^{14}C ages, 1σ for the varve ^{14}C ages, and a $k=1.3$ error multiplier for both) and ranges from an average 100 ^{14}C yr for the 13,000–12,000 cal BP interval to 300 ^{14}C yr for the 24,000–20,000 cal BP interval.

In its simplest form, the calibration process is a straightforward reading of the calibration curves (Stuiver and Pearson 1993). Because Figures A and B lack uncertainty estimates, we recommend the use of computer programs that include the error margin for age calibration. Computer programs (*e.g.*, CALIB, Stuiver and Reimer 1993; cal15, van der Plicht 1993; and OxCal v2.18, Bronk Ramsey 1994) also generate additional information, such as probability distributions *vs.* cal age. To avoid confusion, we recommend that all computer programs, as of 1999, incorporate the INTCAL98 database for marine and terrestrial age calibration. The INTCAL98 calibration data (atmospheric as well as marine, with one standard deviation uncertainty), the atmospheric $\Delta^{14}C$ and residual $\Delta^{14}C$ values, the CALIB 4.0 computer program based on INTCAL98 data, and $\delta^{18}O$ of the GISP2 ice core can be downloaded from the Quaternary Isotope Laboratory web site at <http://depts.washington.edu/qil/>.

https://doi.org/10.1017/S0033822200019123 Published online by Cambridge University Press

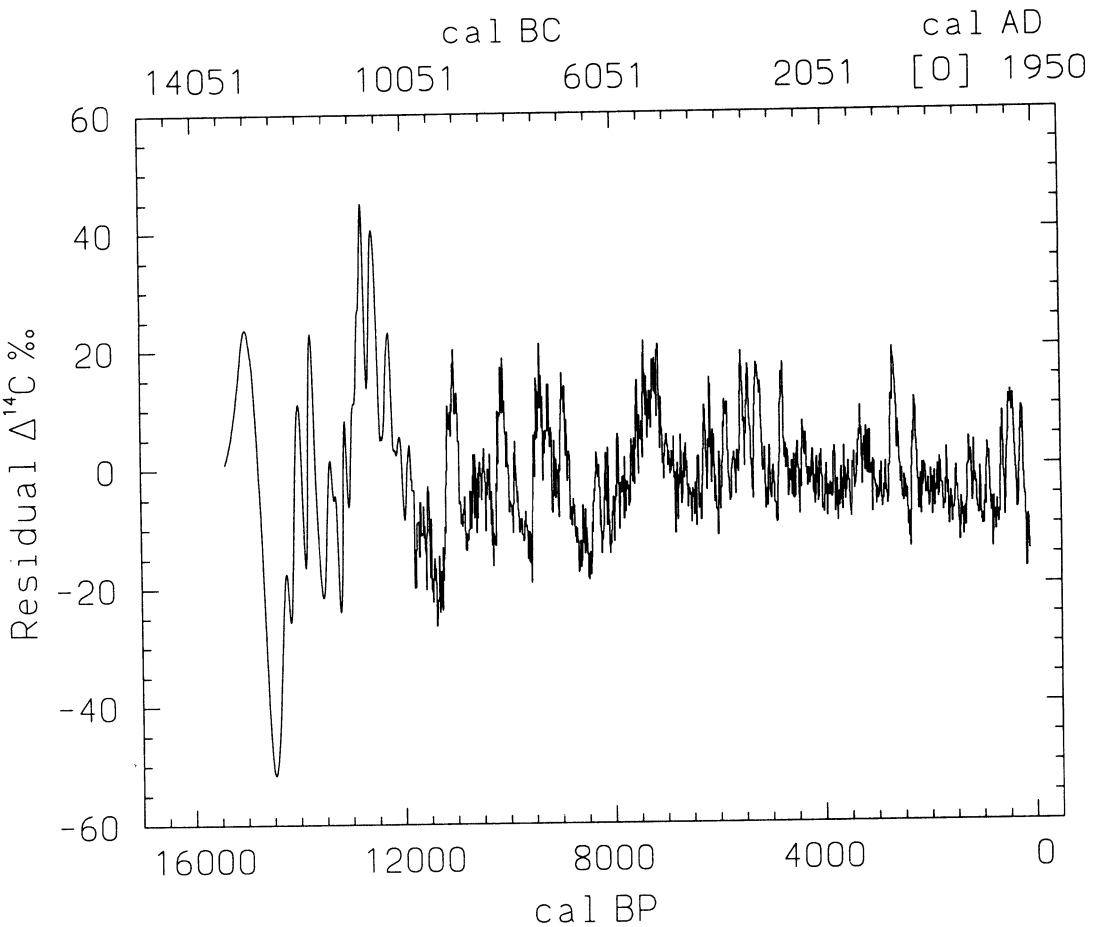

Fig. 13. $\Delta^{14}C$ residual variations, after removing a 2000-yr moving average from the Fig. 12 profile

ACKNOWLEDGMENTS

Both the above radiocarbon age synthesis, and the radiocarbon age measurement program of the Seattle laboratory, were funded by the National Science Foundation (NSF) grant ATM-9310121 to M. Stuiver. Research of E. Bard was supported by IUF, CNRS and EC grants; J. W. Beck and G. S. Burr's research was supported by grants OCE-9402693, OCE-9500647, OCE-9501580, OCE-9503256, EAR-9508413, EAR-8904987, EAR-9512334, EAR-9406183, ATM-8922114 (all NSF), NOAA(NAS6QP0381), and ORSTOM. Cariaco basin research (K. O. Hughen) was funded by the U.S. Department of Energy (contract W-7405-ENG-48), a NASA Earth System Science Fellowship, OCE-9521058 (NSF), and NOAA. Heidelberg radiocarbon research (B. Kromer) was funded by the German Science Foundation (DFG) and the Ministry of Science and Research (BMBF). Support for the Belfast laboratory (G. McCormac) was through NERC, grant GR9/02597. The dendrochronological research at Hohenheim (M. Spurk) was supported by the European Commission (ENV4-CT95-0127-PL951087) and BMF 07VKV/01A -21178.3/3.

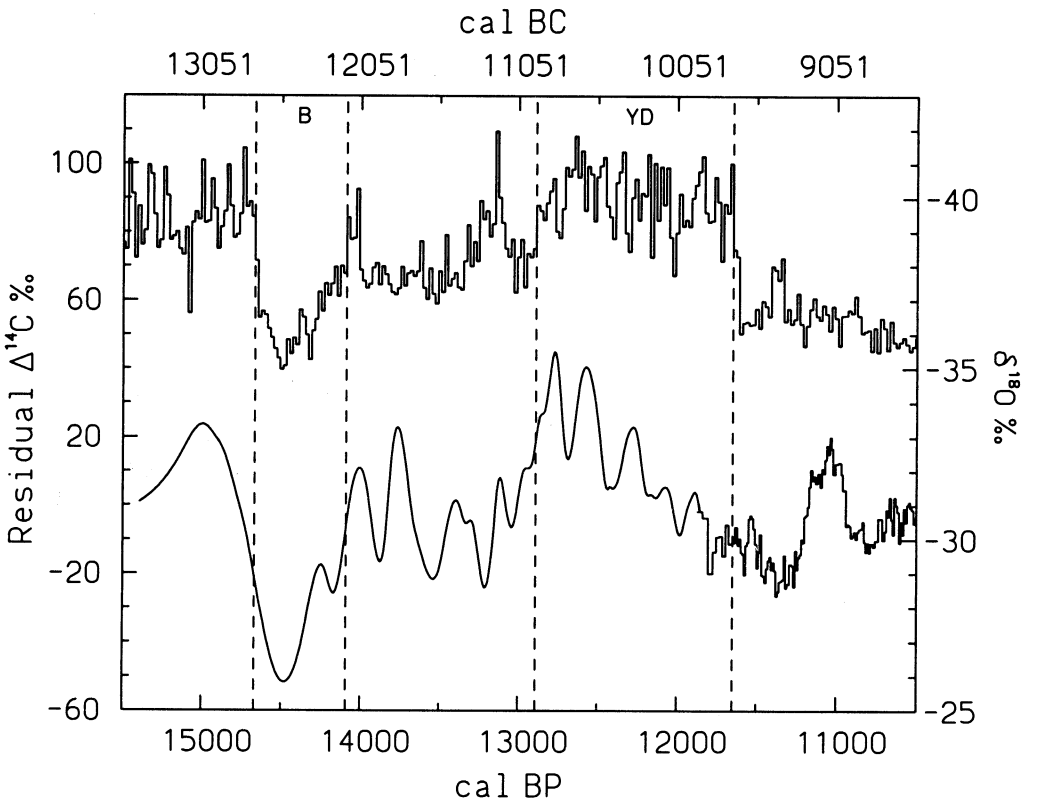

Fig. 14. The upper curve depicts the inverted GISP2 oxygen isotope ratio ($\delta^{18}O$) record with bidecadal time separation (Stuiver, Grootes and Braziunas 1995). The lower curve is based on INTCAL98 residual $\Delta^{14}C$. The cal BP scale of the oxygen isotope record is based on ice layer counts (Alley *et al.* 1997). B = Bølling, YD = Younger Dryas.

REFERENCES

Adkins, J. F., Cheng, H., Boyle, E. A., Druffel, E. R. M. and Edwards, R. L. 1998 Deep-sea coral evidence for rapid change in ventilation of the deep North Atlantic 15,400 years ago. *Science* 280: 725–728.

Alley, R. B., Shuman, C. A., Meese, D. A., Gow, A. J., Taylor, K. C., Cuffey, K. M., Fitzpatrick, J. J., Grootes, P. M., Zielinski, G. A., Ram, M., Spinelli, G. and Elder, B. 1997 Visual-stratigraphic dating of the GISP2 core: Basis, reproducibility, and application. *Journal of Geophysical Research* 102(C12): 26,370–26,381.

Bard, E. 1988 Correction of accelerator mass spectrometry ^{14}C ages measured in planktonic foraminifera: Paleoceanographic implications. *Paleoceanography* 3: 635–645.

Bard, E., Arnold, M., Hamelin, B., Tisnerat-Laborde, N. and Cabioch, G. 1998 Radiocarbon calibration by means of mass spectrometric $^{230}Th/^{234}U$ and ^{14}C ages of corals: An updated database including samples from Barbados, Mururoa and Tahiti. *Radiocarbon*, this issue.

Bard, E., Arnold, M., Mangerud, M., Paterne, M., Labeyrie, L., Duprat, J., Mélières, M. A., Sonstegaard, E. and Duplessy, J. C. 1994 The North Atlantic atmosphere-sea surface ^{14}C gradient during the Younger Dryas climatic event. *Earth and Planetary Science Letters* 126: 275–287.

Bard, E., Hamelin, B., Fairbanks, R. G. and Zindler, A. 1990 Calibration of the ^{14}C timescale over the past 30,000 years using mass spectrometric U-Th ages from Barbados corals. *Nature* 345: 405–410.

Braziunas, T. F., Fung, I. E. and Stuiver, M. 1995 The preindustrial atmospheric $^{14}CO_2$ latitudinal gradient as related to exchanges among atmospheric, oceanic, and terrestrial reservoirs. *Global Biogeochemical Cycles* 9: 565–584.

Broecker, W. S. 1997 Thermohaline circulation, the Achilles heel of our climate system: Will man-made CO_2 upset the current balance? *Science* 278: 1582–1588.

____1998 Paleocean circulation during the last glaciation: A bipolar seesaw? *Paleoceanography* 13: 119–121.

https://doi.org/10.1017/S0033822200019123 Published online by Cambridge University Press

Bronk Ramsey, C. 1994 Analysis of chronological information and radiocarbon calibration: The program OxCal. *Archaeological and Computing Newsletter* 41: 11–16.

Burr, G. S., Beck, J. W., Taylor, F. W., Récy, J., Edwards, R. L. Cabioch, G., Corrège, T., Donahue, D. J. and O'Malley, J. M. 1998 A high-resolution radiocarbon calibration between 11,700 and 12,400 calendar years BP derived from ^{230}Th ages of corals from Espiritu Santo Island, Vanuatu. *Radiocarbon*, this issue.

Damon, P. E. 1995 A note concerning "Location-dependent differences in the ^{14}C content of wood" by McCormac *et al. In* Cook, G. T., Harkness, D. D., Miller, B. F. and Scott, E. M., eds., Proceedings of the 15th International ^{14}C Conference. *Radiocarbon* 37(2): 829–830.

Damon, P. E., Burr, G., Peristykh, A. N., Jacoby, G. C. and D'Arrigo, R. D. 1996 Regional radiocarbon effect due to thawing of frozen earth. *Radiocarbon* 38(3): 597–602.

Edwards, R. L., Beck, J. W., Burr, G. S., Donahue, D. J., Chappell, J. M. A., Bloom, A. L., Druffel, E. R. M. and Taylor, F. W. 1993 A large drop in atmospheric ^{14}C/^{12}C and reduced melting in the Younger Dryas, documented with ^{230}Th ages of corals. *Science* 260: 962–968.

Hughen, K. A., Overpeck, J. T., Lehman, S. J., Kashgarian, M., Southon, J., Peterson, L. C., Alley, R. and Sigman, D. M. 1998 Deglacial changes in ocean circulation from an extended radiocarbon calibration. *Nature* 391: 65–68.

Kitagawa, H. and van der Plicht, J. 1998 Atmospheric radiocarbon calibration to 45,000 yr B.P.: Late Glacial fluctuations and cosmogenic isotope production. *Science* 279: 1187–1190.

Kromer, B., Rhein, M., Bruns, M., Schoch-Fischer, H., Münnich, K. O., Stuiver, M. and Becker, B. 1986 Radiocarbon calibration data for the 6th to the 8th millennia BC. *In* Stuiver, M. and Kra, R., eds., Calibration Issue. *Radiocarbon* 28(2B): 954–960.

Kromer, B. and Spurk, M. 1998 Revision and tentative extension of the tree-ring based ^{14}C calibration, 9200–11,855 cal BP. *Radiocarbon,* this issue.

Lal, D. 1985 Carbon cycle variations during the past 50.000 years: Atmospheric ^{14}C/^{12}C ratio as an isotopic indicator. *In* Sundquist, E. T. and Broecker, W. S., eds., *The Carbon Cycle and Atmospheric CO_2: Natural Variations, Archean to Present.* Geophysical Monograph 32. Washington, D.C., American Geophysical Union: 221–233.

Mangini, A., Lomitschka, M., Eichstädter, R., Frank, N. and Vogler, S. 1998 Coral provides way to age deep water. *Nature* 392: 347–348.

McCormac, F. G., Baillie, M. G. L., Pilcher, J. R. and Kalin, R. M. 1995 Location-dependent differences in the ^{14}C content of wood. *In* Cook, G. T., Harkness, D. D., Miller, B. F. and Scott, E. M., eds., Proceedings of the 15th International ^{14}C Conference. *Radiocarbon* 37(2): 395–407.

McCormac, F. G., Hogg, A. G., Higham, T. F. G., Baillie, M. G. L., Palmer, J. G., Xiong, L., Pilcher, J. R., Brown, D. and Hoper, S. T. 1998a Variations of radiocarbon in tree rings: Southern Hemisphere offset preliminary results. *Radiocarbon,* this issue.

McCormac, F. G., Hogg, A. G., Higham, T. F. G., Lynch-Stieglitz, J., Broecker, W. S., Baillie, M. G. L., Palmer, J., Xiong, L., Pilcher, J. R., Brown, D. and Hoper S. T. 1998b Temporal variation in the interhemispheric ^{14}C offset. *Geophysical Research Letters* 25: 1321–1324.

Pearson, G. W., Becker, B. and Qua, F. 1993 High-precision ^{14}C measurement of German and Irish oaks to show the natural ^{14}C variations from 7890 to 5000 BC. *In* Stuiver, M., Long, A. and Kra, R. S., eds., Calibration 1993. *Radiocarbon* 35(1): 93–104.

Pearson, G. W. and Stuiver, M. 1993 High-precision bidecadal calibration of the radiocarbon time scale, 500–2500 BC. *In* Stuiver, M., Long, A. and Kra, R. S., eds., Calibration 1993. *Radiocarbon* 35(1): 25–33.

Pilcher, J. R., Baillie, M. G. L., Schmidt, B. and Becker, B. 1984 A 7,272-year tree-ring chronology for Western Europe. *Nature* 312: 150–152.

Reinsch, C. H. 1967 Smoothing by spline functions. *Numerische Mathematik* 10: 177–183.

Spurk, M., Friedrich, M., Hofmann, J., Remmele, S., Frenzel, B., Leuschner, H. H. and Kromer, B. 1998 Revisions and extension of the Hohenheim oak and pine chronologies: New evidence about the timing of the Younger Dryas / Preboreal transition. *Radiocarbon,* this issue.

Stuiver, M. 1982 A high-precision calibration of the AD radiocarbon time scale. *Radiocarbon* 24(1): 1–26.

Stuiver, M. and Becker, B. 1986 High-precision decadal calibration of the radiocarbon time scale, AD 1950–2500 BC. *In* Stuiver, M. and Kra, R., eds., Calibration Issue. *Radiocarbon* 28(2B): 863–910.

____1993 High-precision decadal calibration of the radiocarbon time scale, AD 1950–6000 BC. *In* Stuiver, M., Long, A. and Kra, R. S., eds., Calibration 1993. *Radiocarbon* 35(1): 35–65.

Stuiver, M. and Braziunas, T. F. 1993 Sun, ocean, climate and atmospheric $^{14}CO_2$: An evaluation of causal and spectral relationships. *The Holocene* 3: 289–305.

____1998 Anthropogenic and solar components of hemispheric ^{14}C. *Geophysical Research Letters* 25: 329–332.

Stuiver, M., Braziunas, T. F., Grootes, P. M. and Zielinski, G. A. 1997 Is there evidence for solar forcing of climate in the GISP2 oxygen isotope record? *Quaternary Research* 48: 259–266.

Stuiver, M., Grootes, P. M. and Braziunas, T. F. 1995 The GISP2 δ^{18}O climate record of the past 16,500 years and the role of the sun, ocean, and volcanoes. *Quaternary Research* 44: 341–354.

Stuiver, M. and Kra, R., eds. 1986 Calibration issue. *Ra-*

diocarbon 28(2B): 805–1030.

Stuiver, M., Long, A. and Kra, R. S., eds. 1993 Calibration 1993. *Radiocarbon* 35(1): 1–244.

Stuiver, M. and Östlund, H. G. 1980 GEOSECS Atlantic radiocarbon. *Radiocarbon* 22(1): 1–24.

Stuiver, M. and Pearson, G. W. 1993 High-precision bidecadal calibration of the radiocarbon time scale, AD 1950–500 BC and 2500–6000 BC. *In* Stuiver, M., Long, A. and Kra, R. S., eds., Calibration 1993. *Radiocarbon* 35(1): 1–23.

Stuiver, M. and Polach, H. A. 1977 Discussion: Reporting of ^{14}C data. *Radiocarbon* 19(3): 355–363.

Stuiver, M. and Quay, P. D. 1981 Atmospheric ^{14}C changes resulting from fossil fuel CO_2 release and cosmic ray flux variability. *Earth and Planetary Science Letters* 53: 349–362.

Stuiver, M. and Reimer, P. J. 1993 Extended ^{14}C data base and revised CALIB 3.0 ^{14}C age calibration program. *In* Stuiver, M., Long, A. and Kra, R. S., eds., Calibration 1993. *Radiocarbon* 35(1): 215–230.

Stuiver, M., Reimer, P. J. and Braziunas, T. F. 1998 High-precision radiocarbon age calibration for terrestrial and marine samples. *Radiocarbon,* this issue.

Toggweiler, J. R., Dixon, K. and Bryan K. 1989 Simulations of radiocarbon in a coarse-resolution world ocean model 1. Steady-state prebomb distributions. *Journal of Geophysical Research* 94: 8217–8242.

van der Plicht, J. 1993 The Groningen radiocarbon calibration program. *In* Stuiver, M., Long, A. and Kra, R. S., eds., Calibration 1993. *Radiocarbon* 35(1): 231–237.

Vogel, J. C., Fuls, A., Visser, E. and Becker, B. 1993 Pretoria calibration curve for short-lived samples, 1930–3350 BC. *In* Stuiver, M., Long, A. and Kra, R. S., eds., Calibration 1993. *Radiocarbon* 35(1): 73–85.

Vogel, J. C. and van der Plicht, J. 1993 Calibration curve for short-lived samples, 1900–3900 BC. *In* Stuiver, M., Long, A. and Kra, R. S., eds., Calibration 1993. *Radiocarbon* 35(1): 87–91.

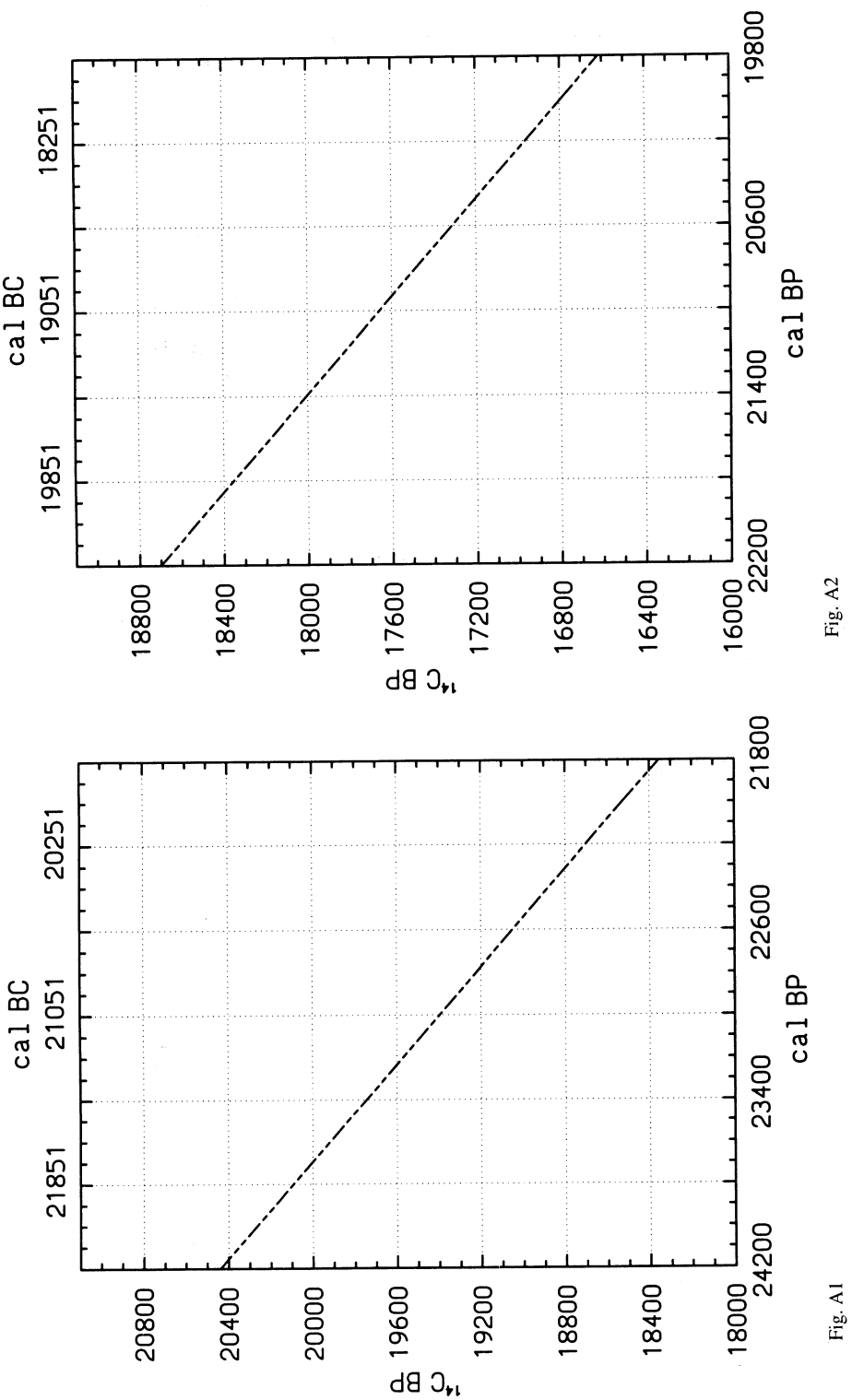

Fig. A1

Fig. A2

Fig. A1–19. INTCAL98 atmospheric calibration curve with decadal resolution back to 11,850 cal BP. The remaining part of INTCAL98 was constructed from coral data with a time resolution of about one century near 12,000 cal BP, and about one millennium near 24,000 cal BP. The dashed portions are based on the splining of a limited number of data points (see Figs. 7 and 8).

https://doi.org/10.1017/S0033822200019123 Published online by Cambridge University Press

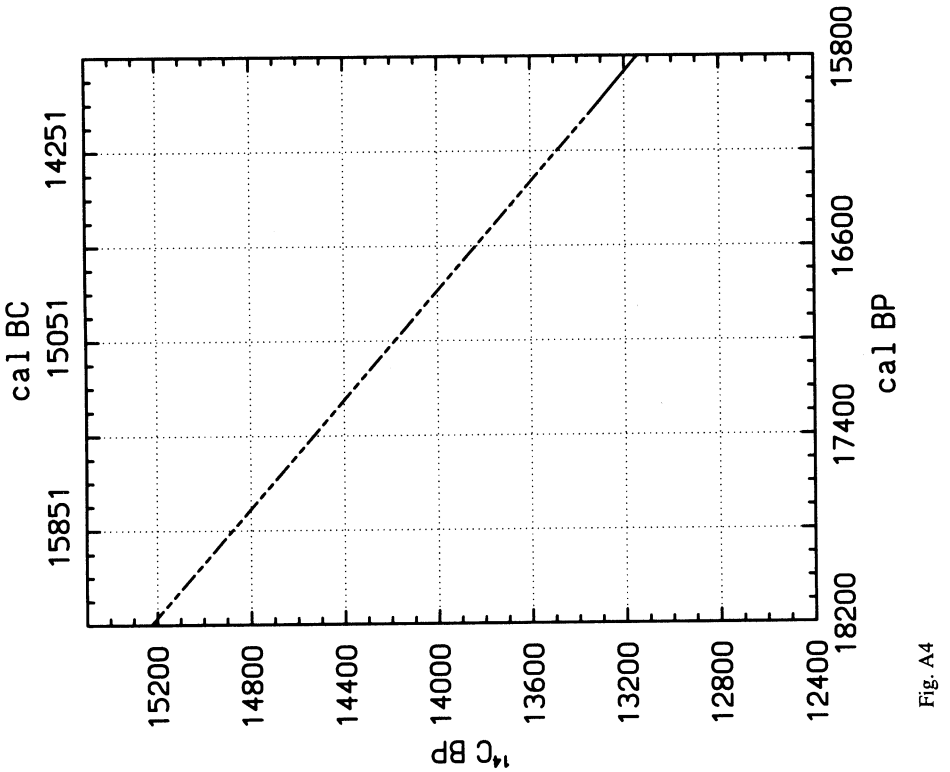

Fig. A4

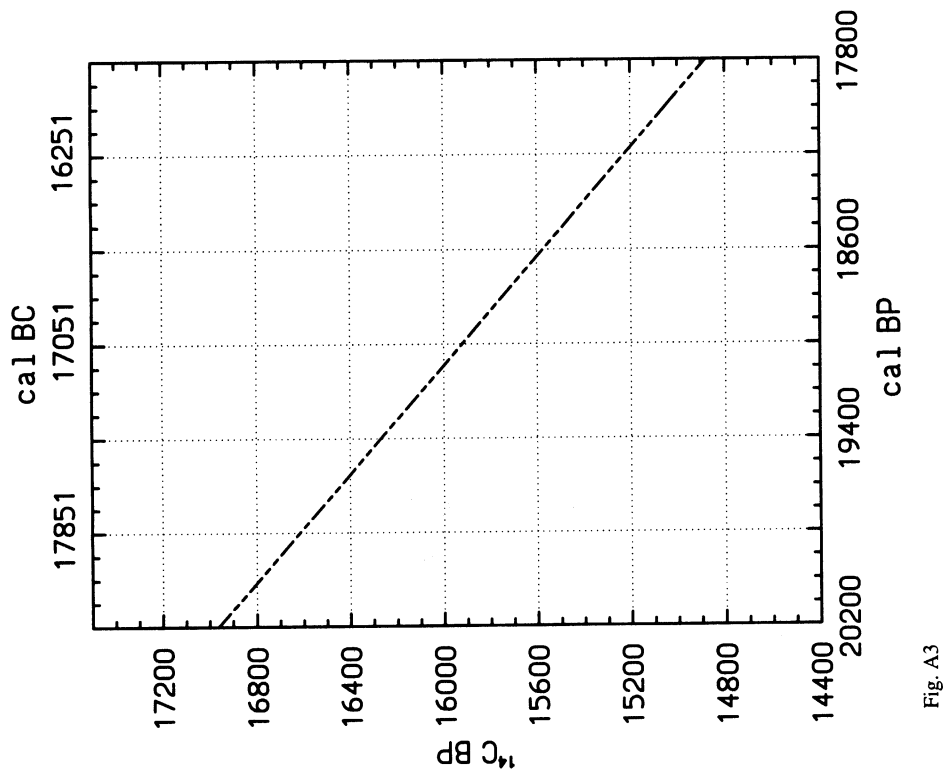

Fig. A3

https://doi.org/10.1017/S0033822200019123 Published online by Cambridge University Press

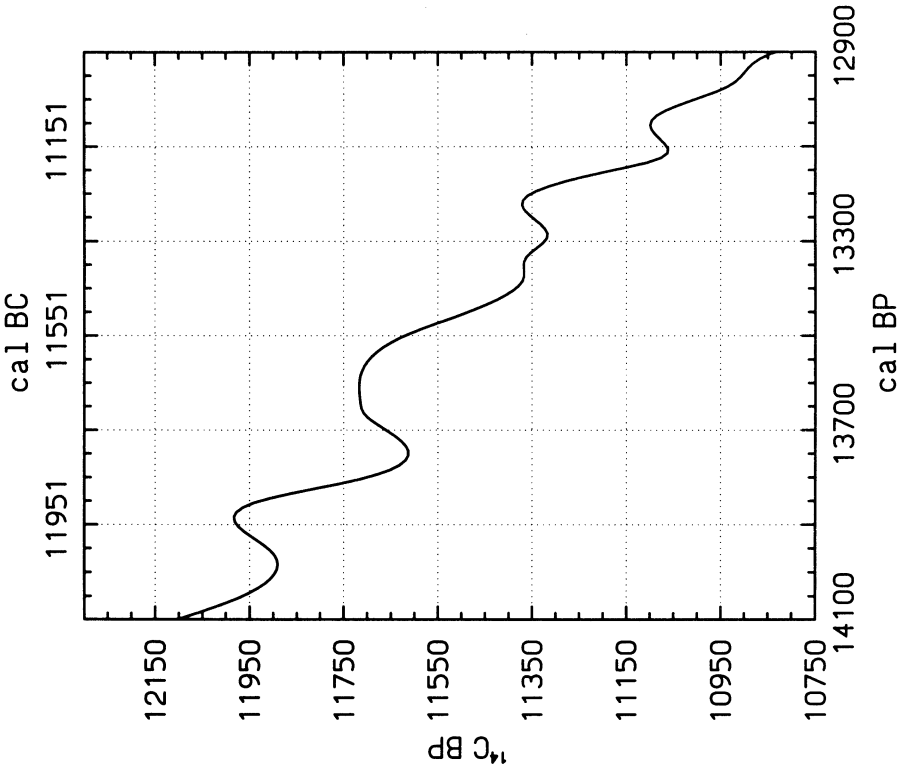

Fig. A6

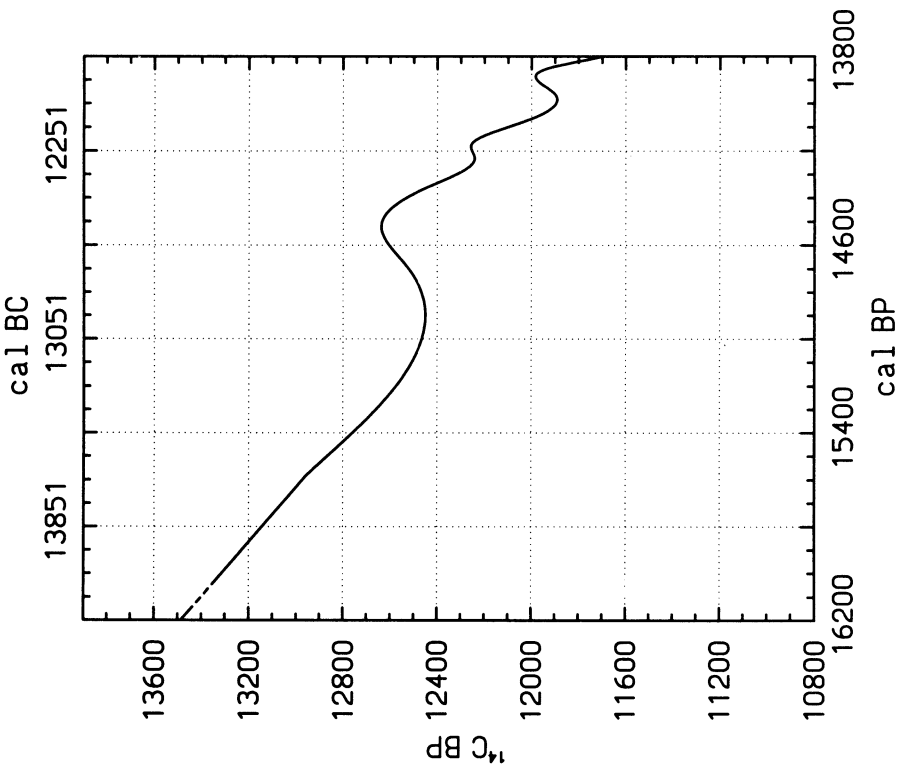

Fig. A5

https://doi.org/10.1017/S0033822200019123 Published online by Cambridge University Press

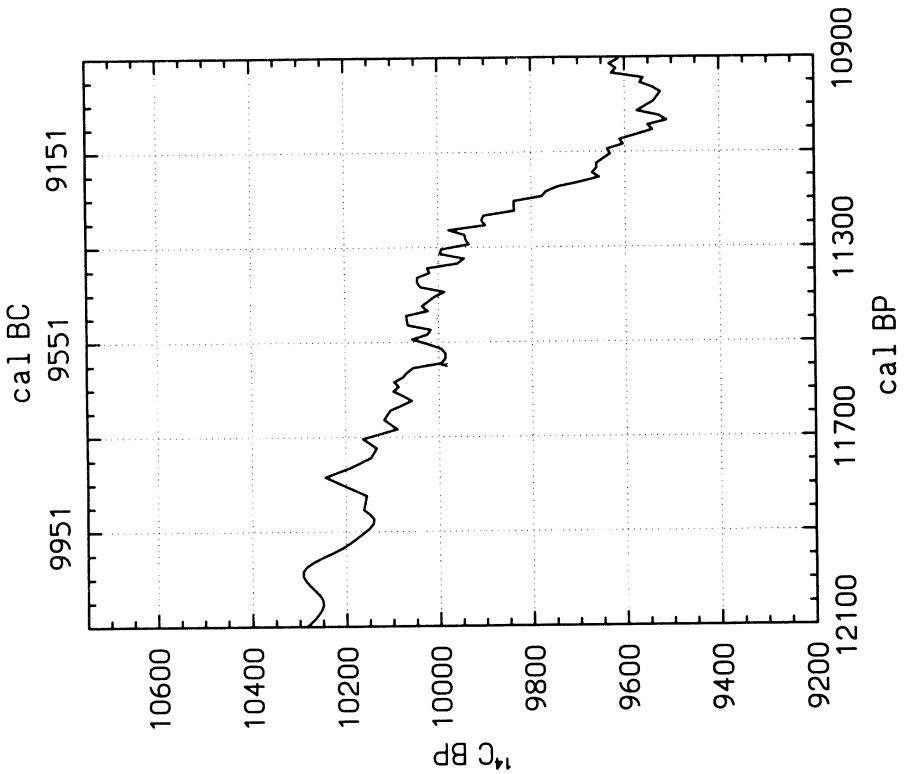

Fig. A8

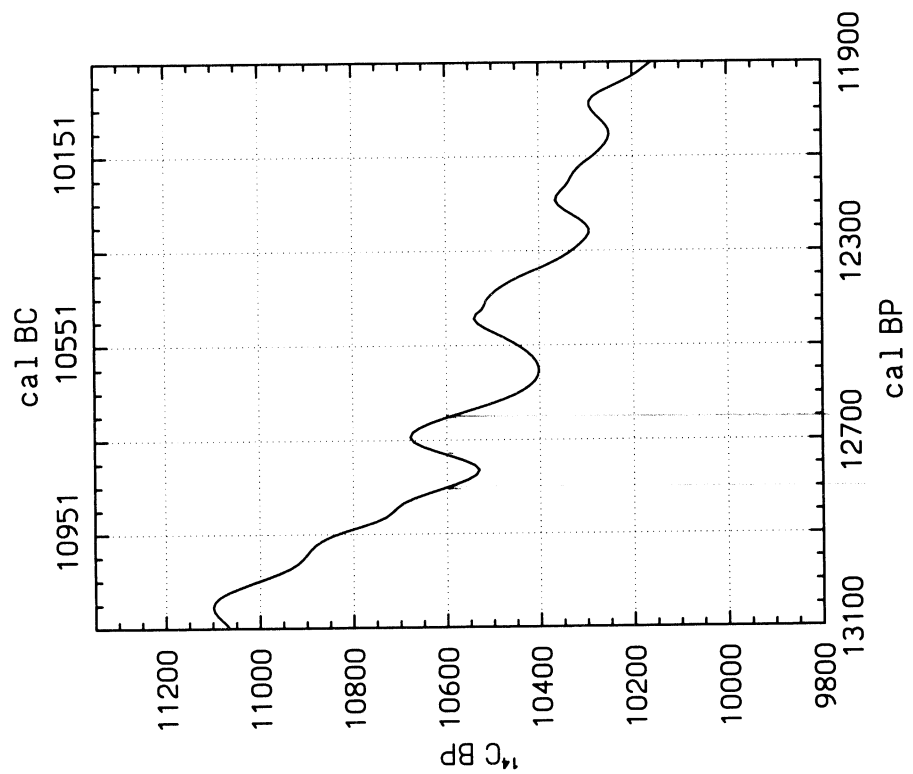

Fig. A7

https://doi.org/10.1017/S0033822200019123 Published online by Cambridge University Press

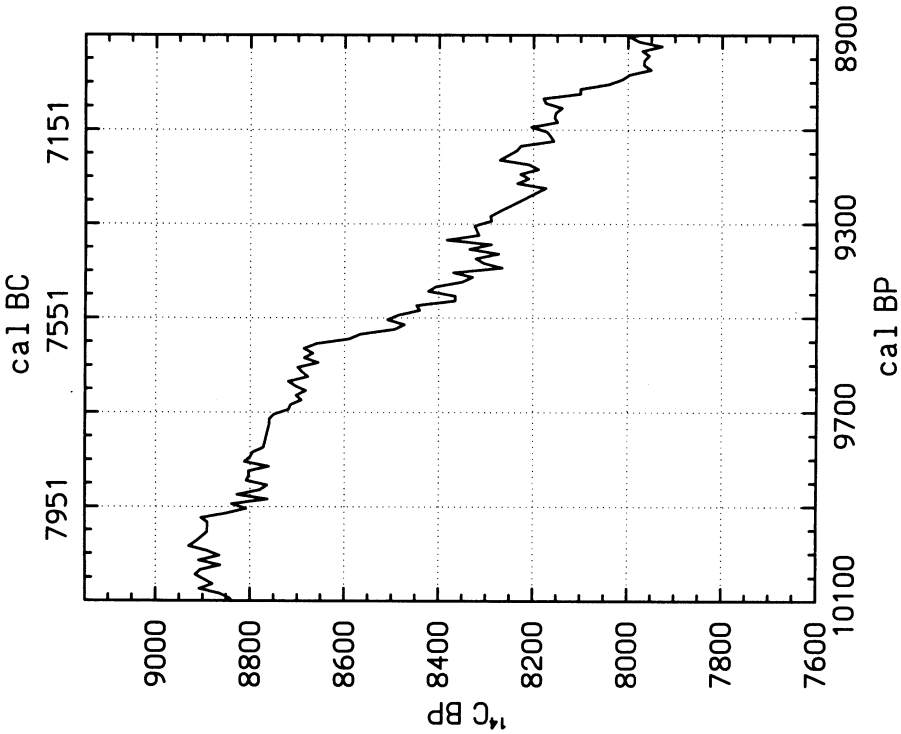

Fig. A10

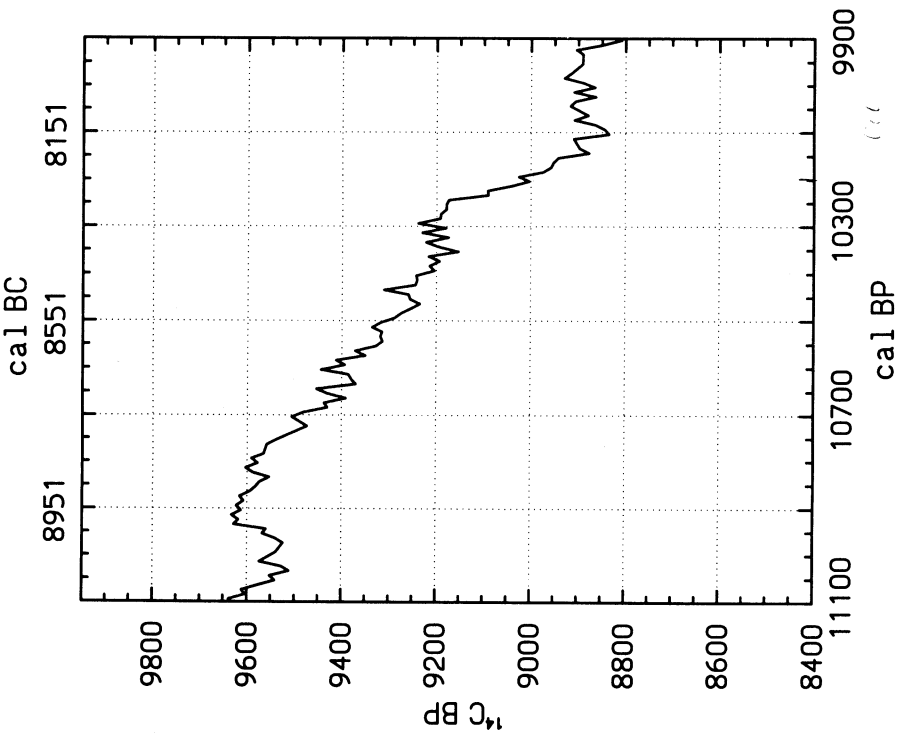

Fig. A9

https://doi.org/10.1017/S0033822200019123 Published online by Cambridge University Press

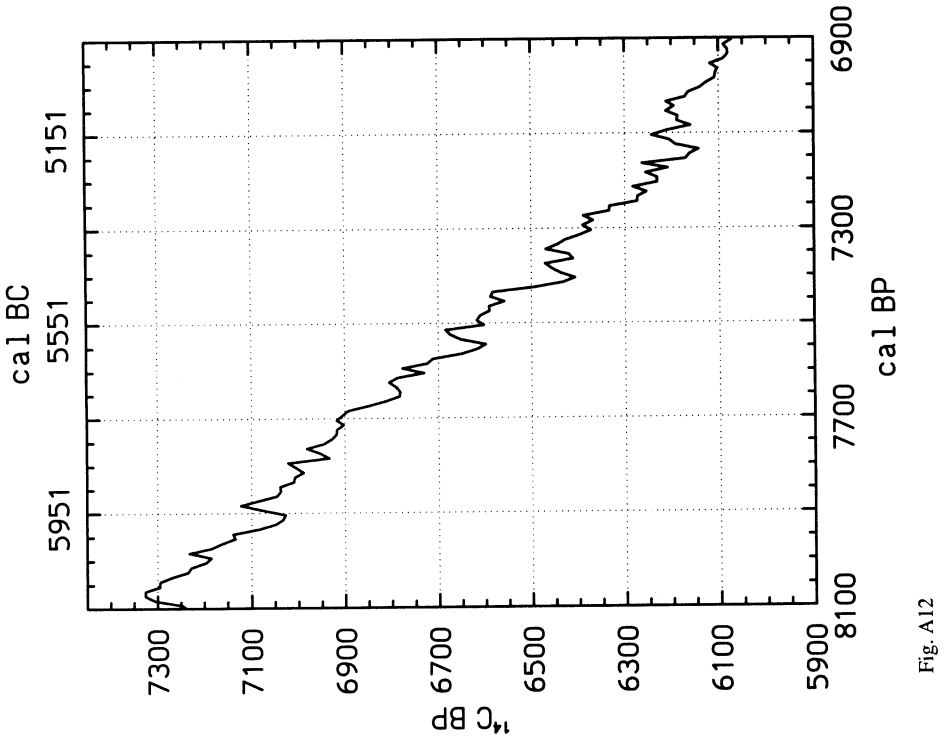

Fig. A12

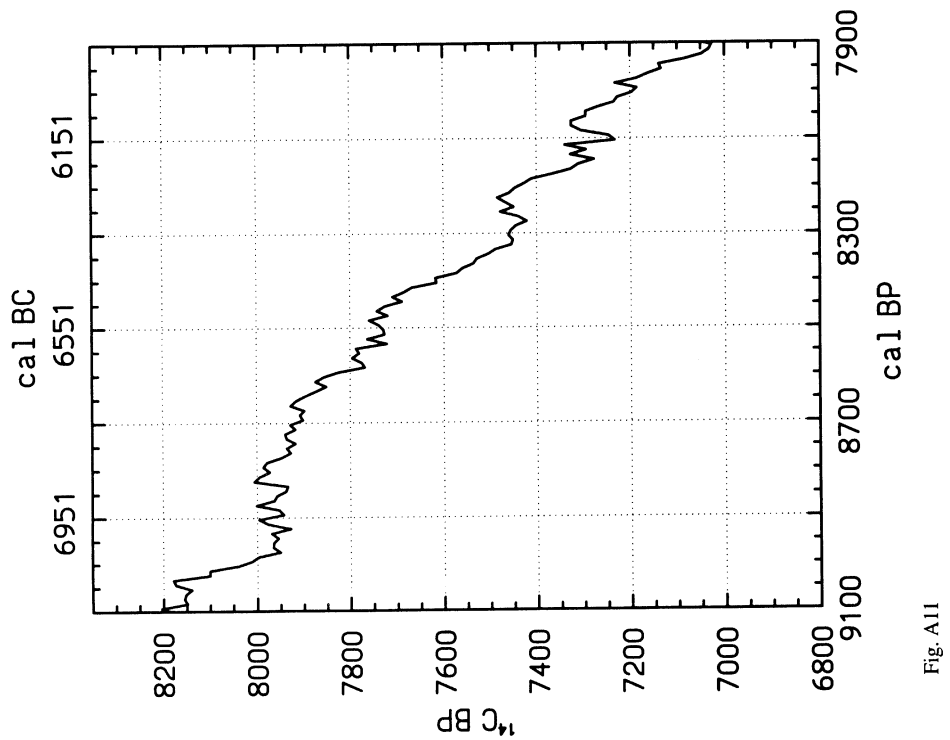

Fig. A11

https://doi.org/10.1017/S0033822200019123 Published online by Cambridge University Press

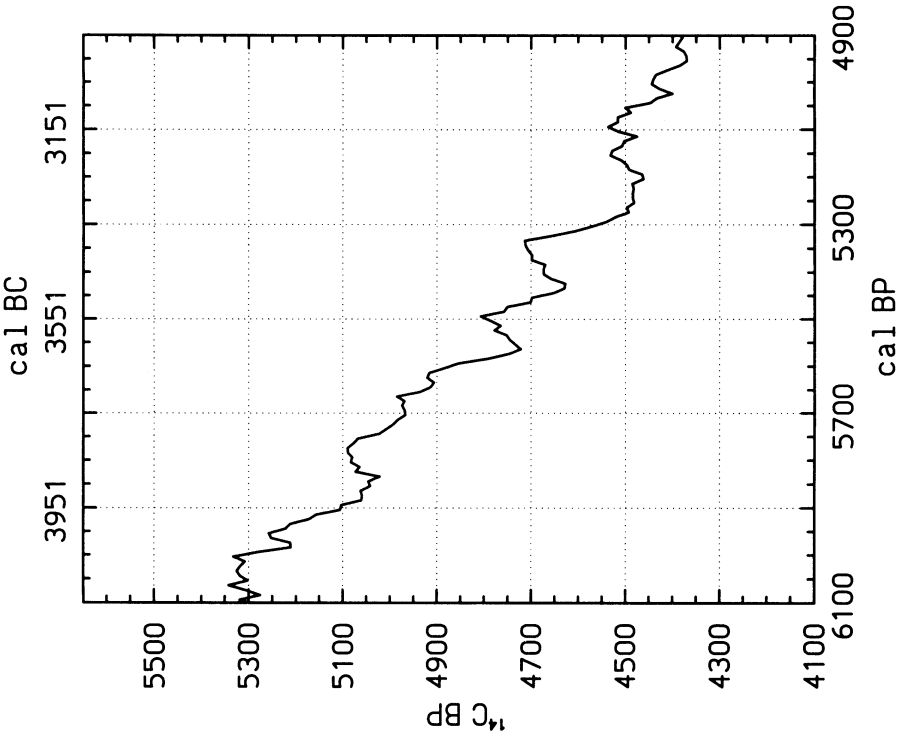

Fig. A14

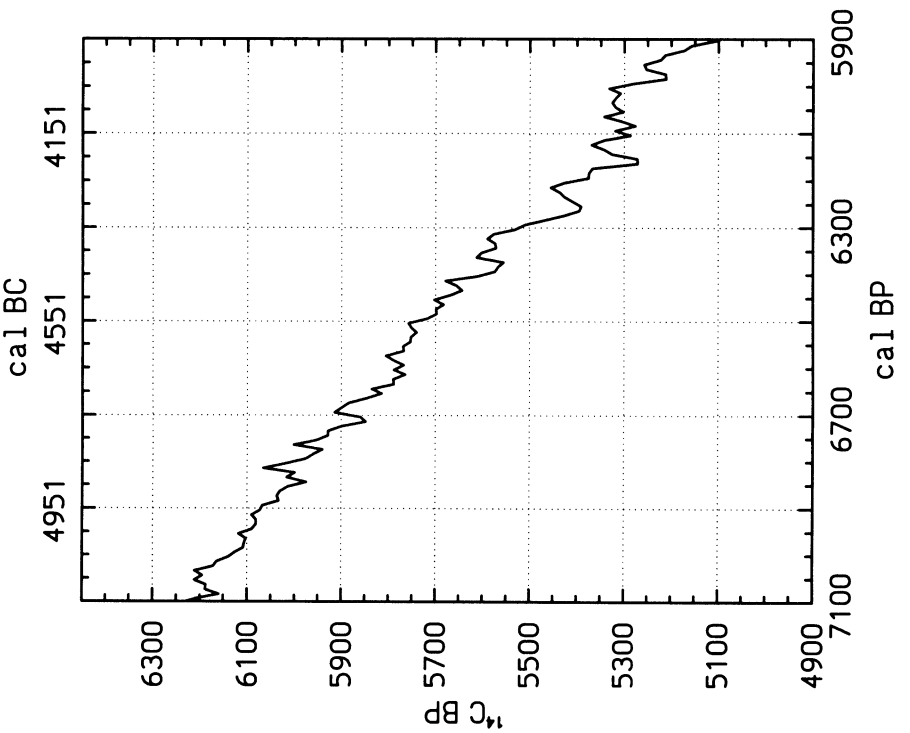

Fig. A13

https://doi.org/10.1017/S0033822200019123 Published online by Cambridge University Press

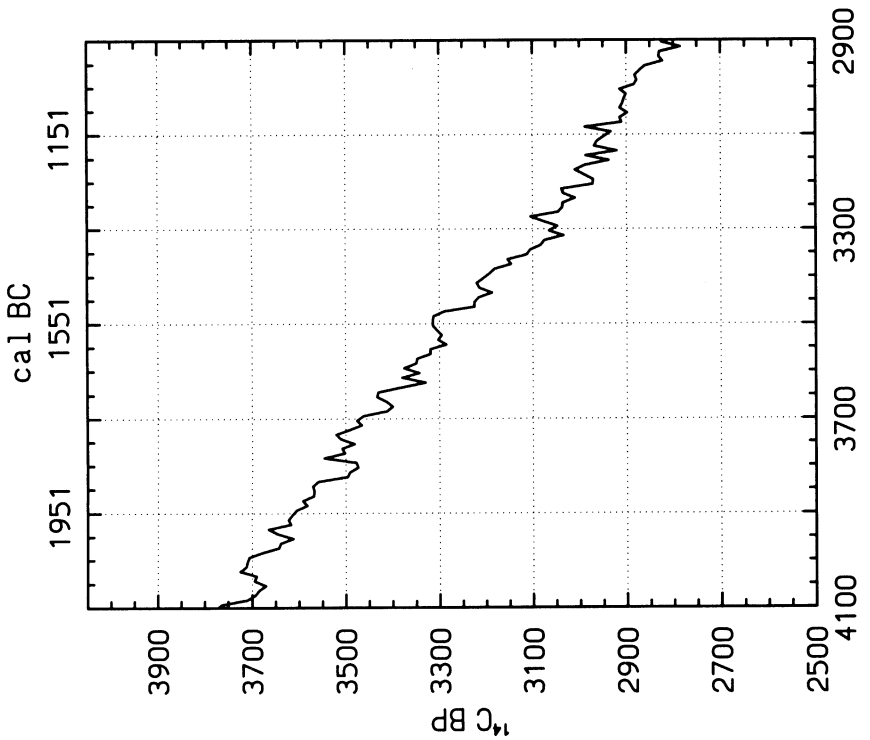

Fig. A16

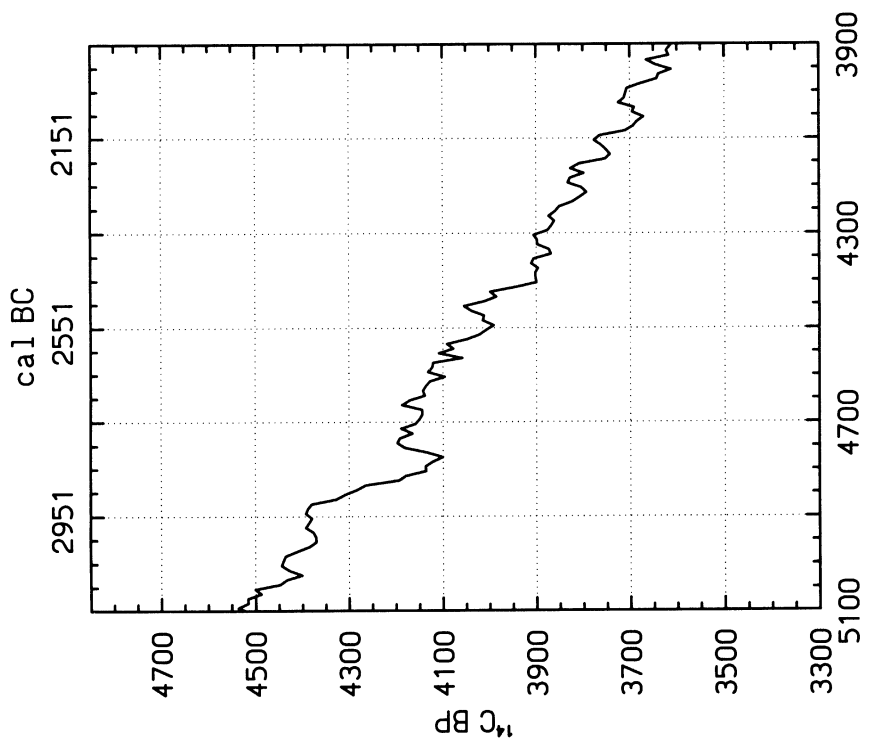

Fig. A15

https://doi.org/10.1017/S0033822200019123 Published online by Cambridge University Press

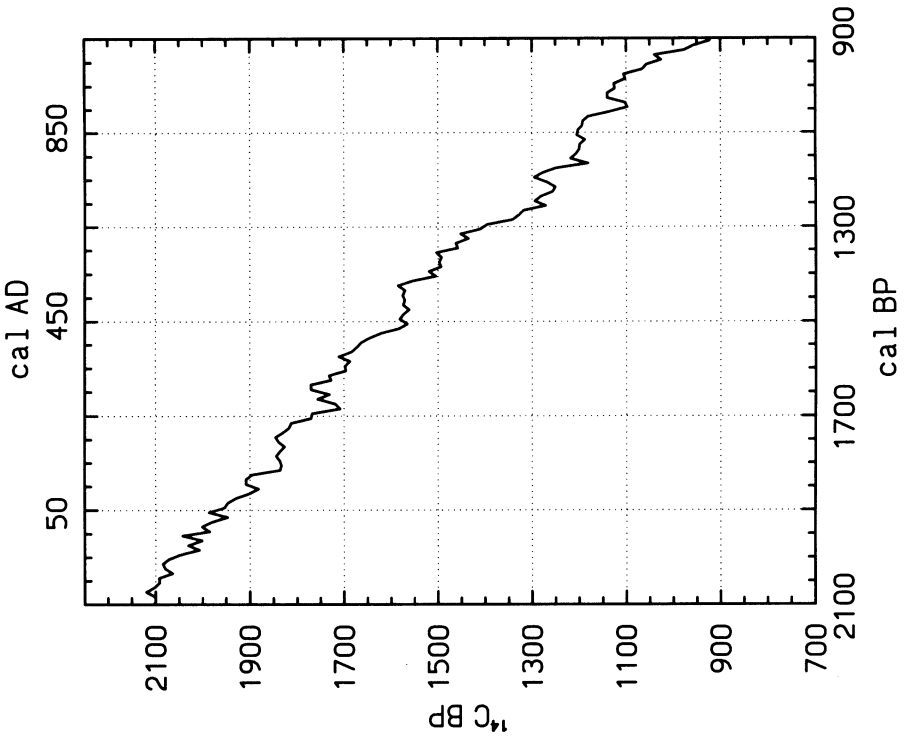

Fig. A18

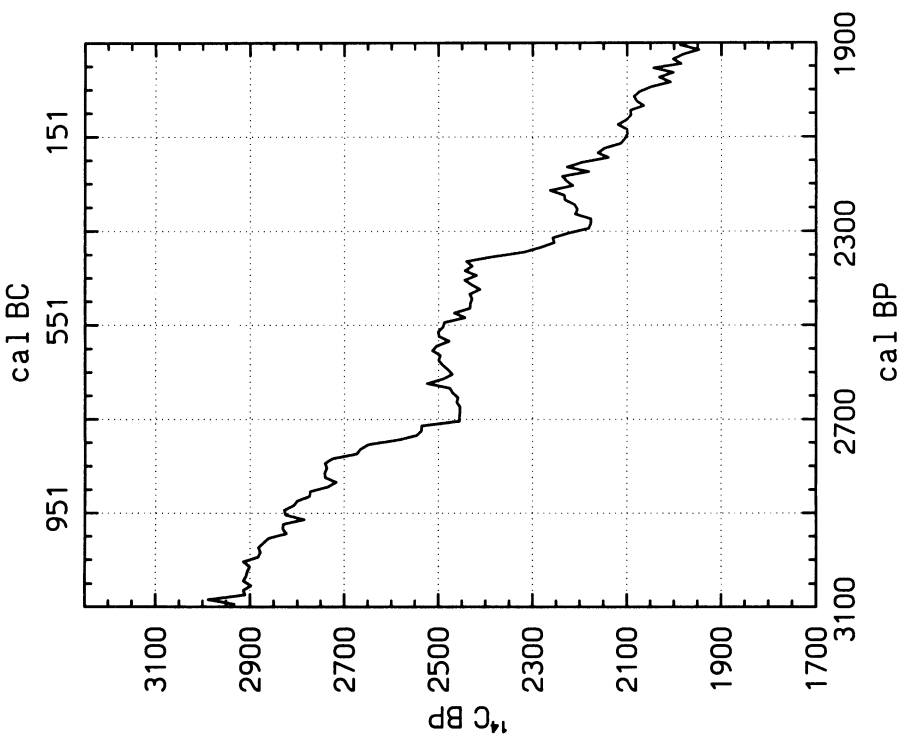

Fig. A17

https://doi.org/10.1017/S0033822200019123 Published online by Cambridge University Press

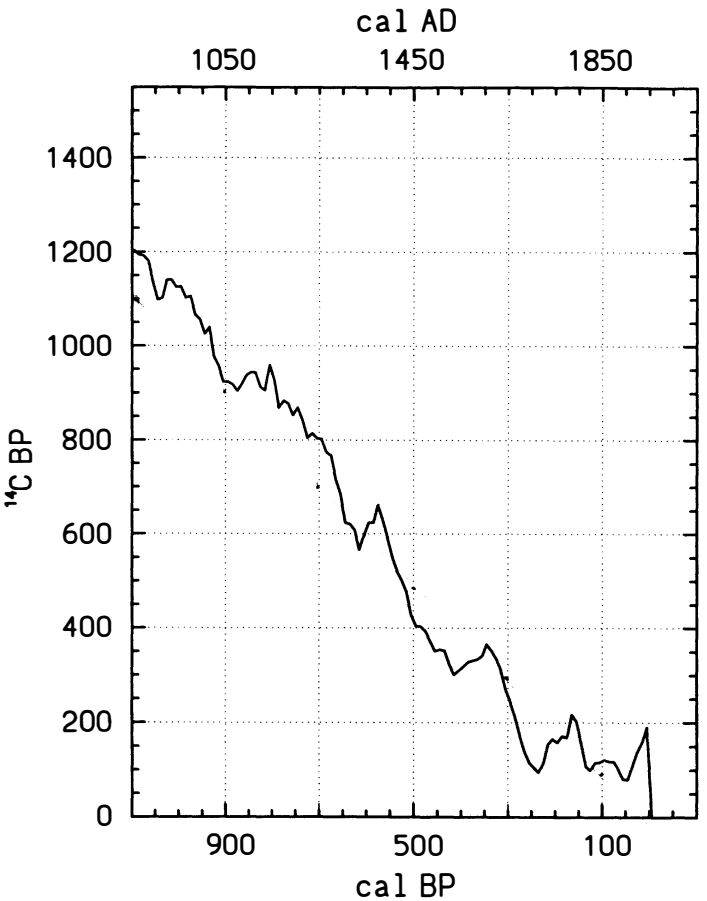

Fig. A19

https://doi.org/10.1017/S0033822200019123 Published online by Cambridge University Press

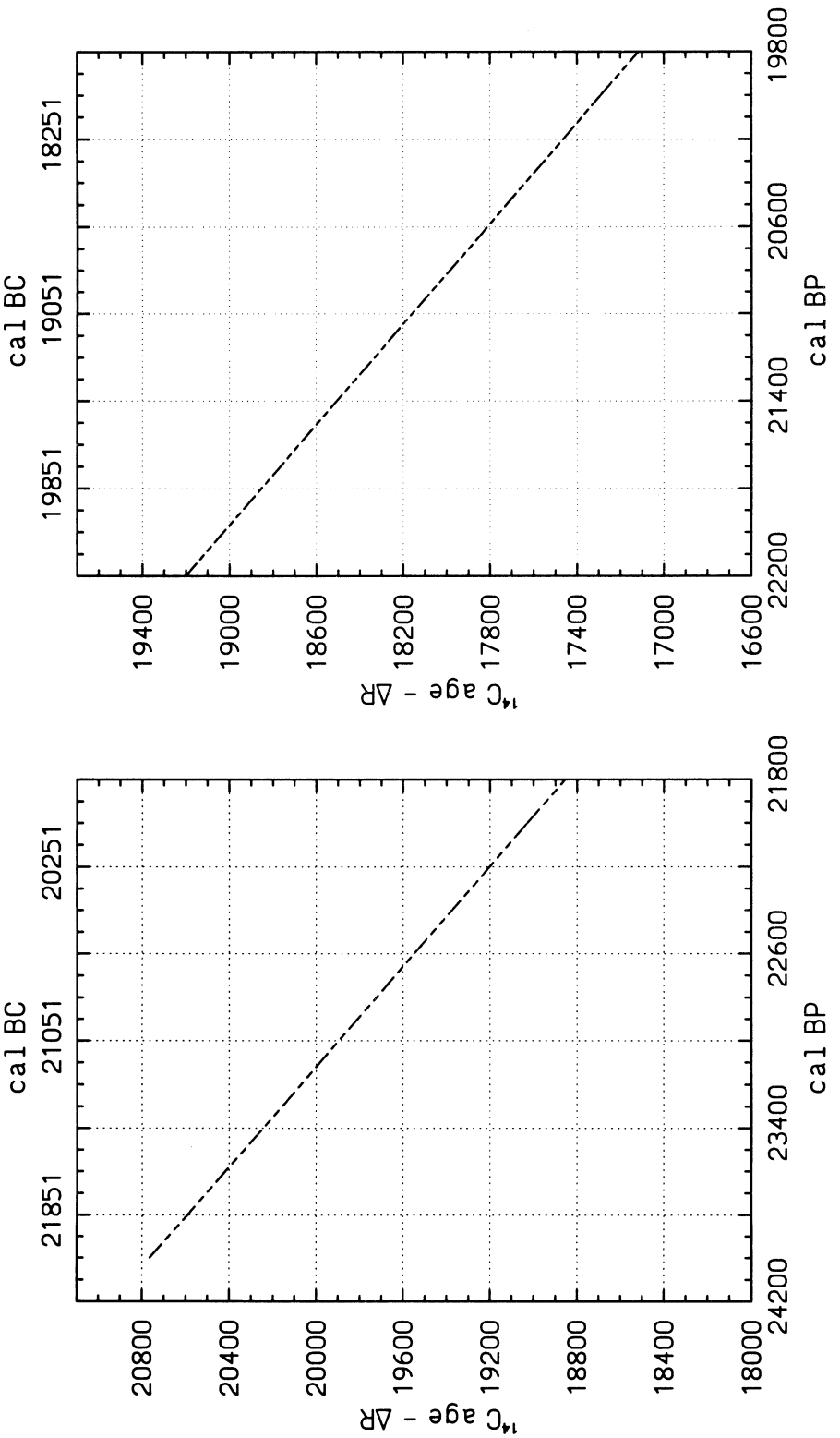

Fig. B2

Fig. B1

Fig. B1–19. INTCAL98 marine calibration curve based on 1) carbon reservoir derived ^{14}C ages for the 8800–0 cal BP interval and 2) coral/varve ^{14}C age determinations for the 8800–24,000 cal BP interval. The dashed portions are based on the splining of a limited number of data points (see Figs. 7 and 8). The very substantial 10,900 cal BP perturbation is dashed because its maximum, generated by a single data point, lacks corroboration.

https://doi.org/10.1017/S0033822200019123 Published online by Cambridge University Press

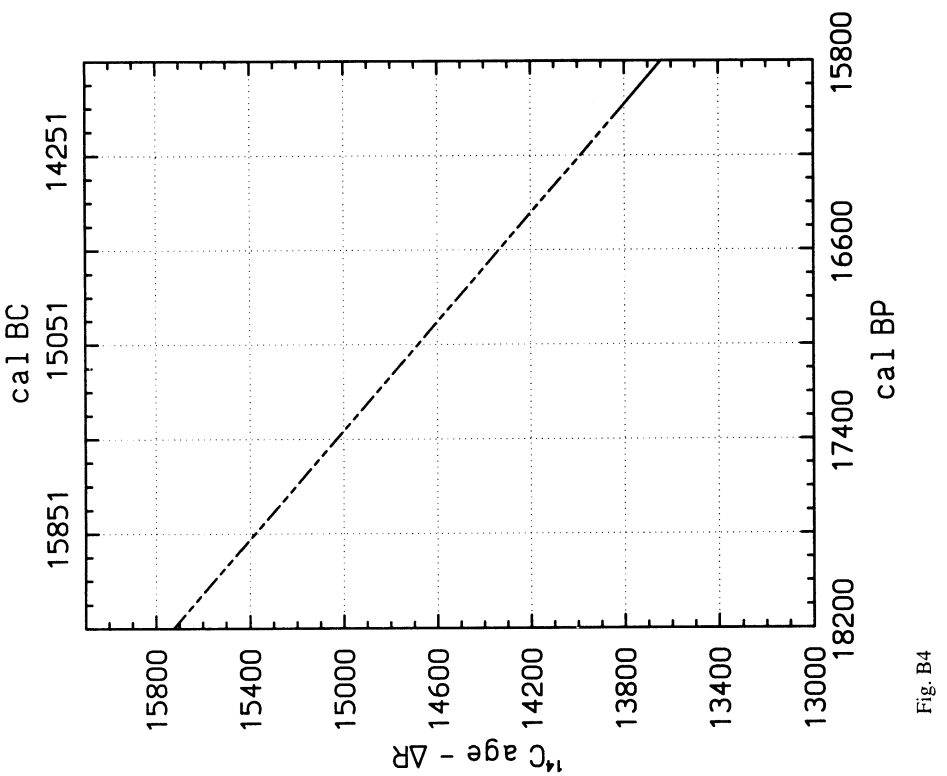

Fig. B4

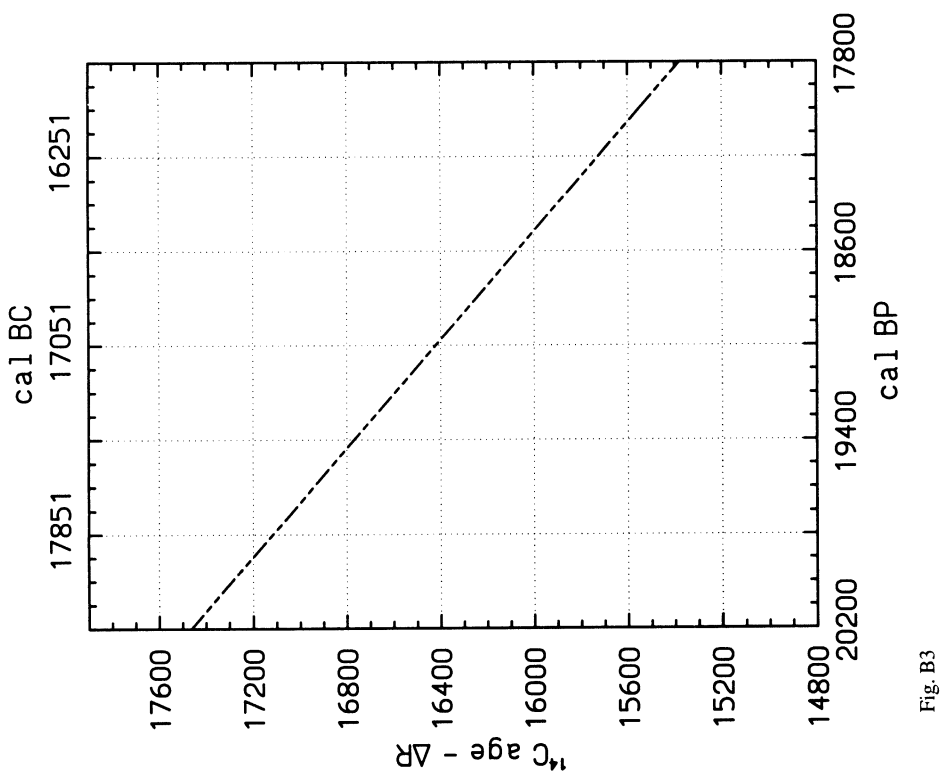

Fig. B3

https://doi.org/10.1017/S0033822200019123 Published online by Cambridge University Press

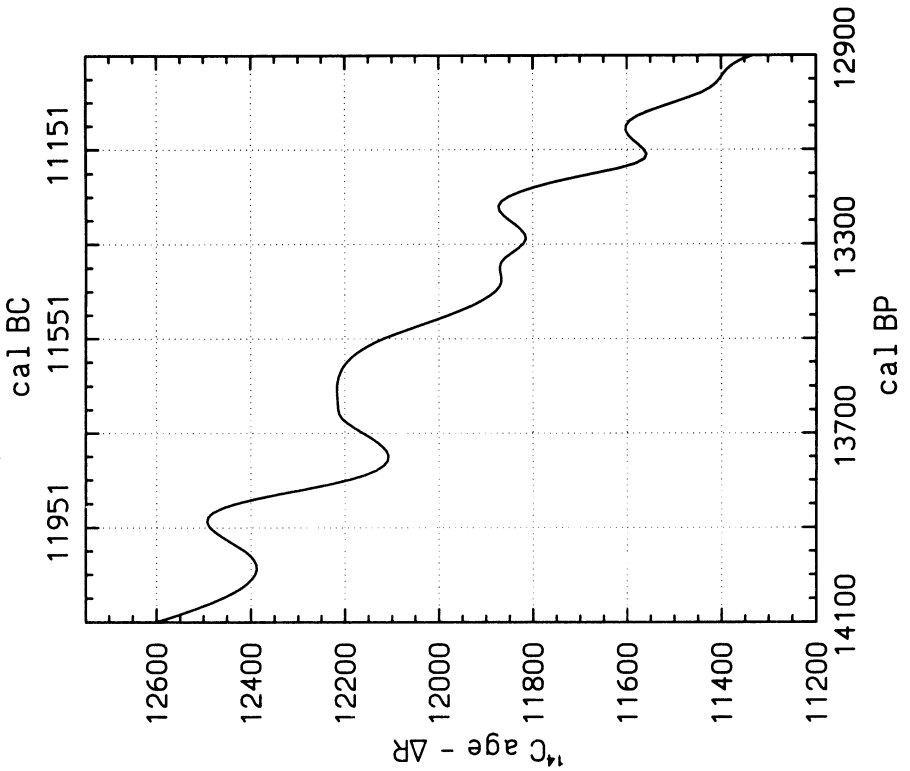

Fig. B6

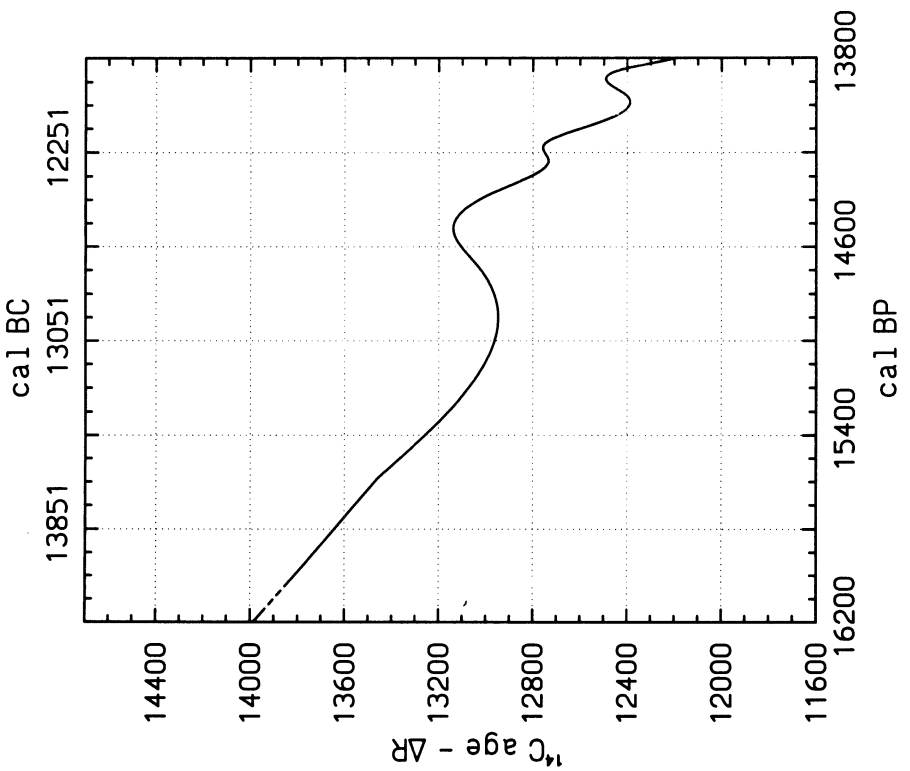

Fig. B5

https://doi.org/10.1017/S0033822200019123 Published online by Cambridge University Press

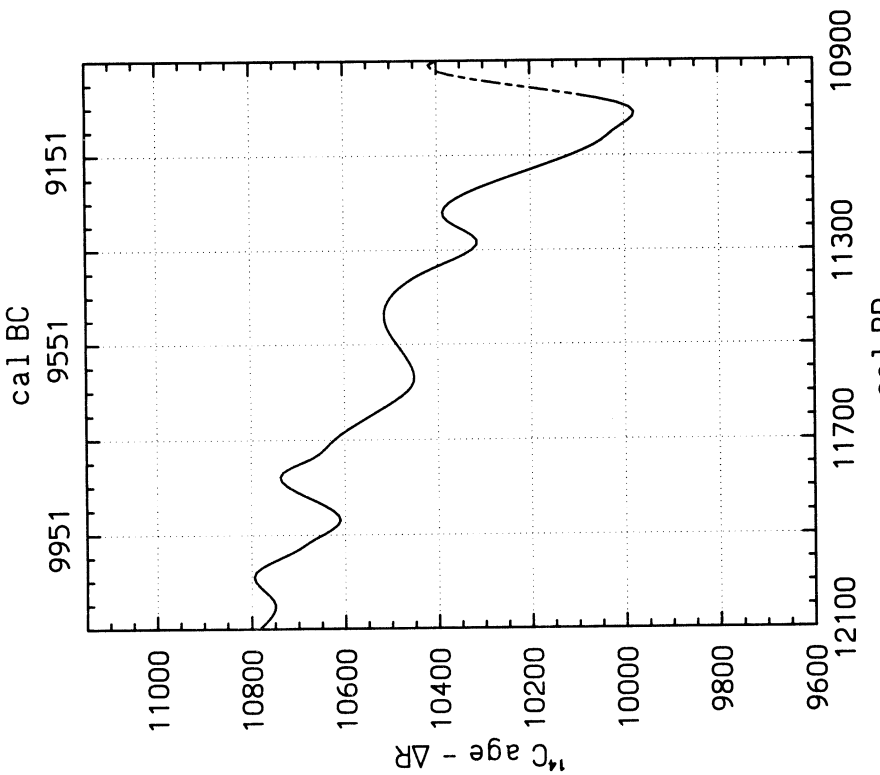

Fig. B8

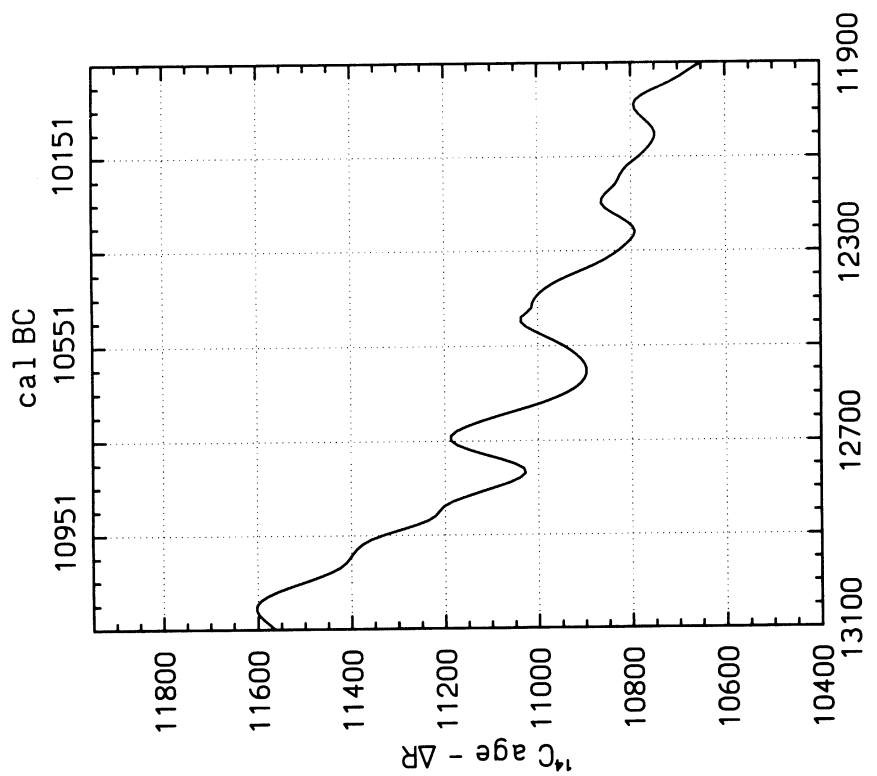

Fig. B7

https://doi.org/10.1017/S0033822200019123 Published online by Cambridge University Press

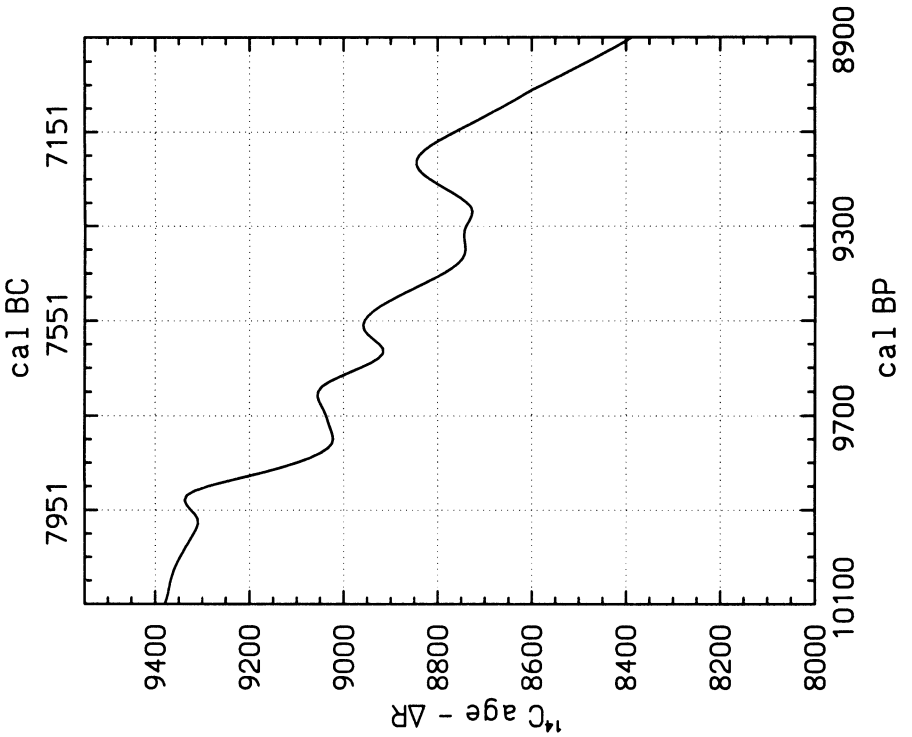

Fig. B10

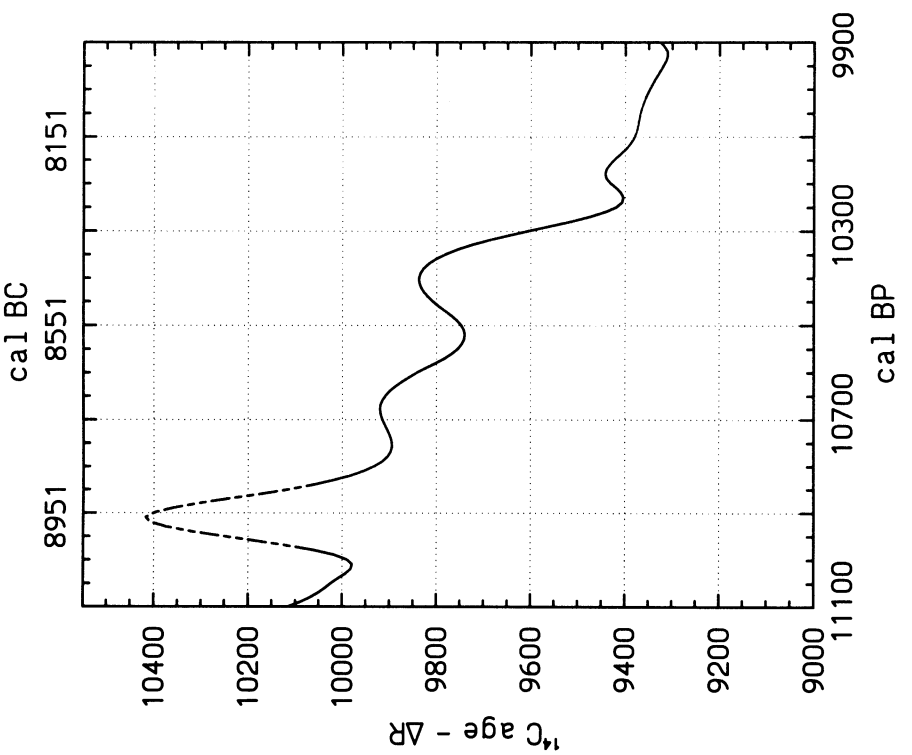

Fig. B9

https://doi.org/10.1017/S0033822200019123 Published online by Cambridge University Press

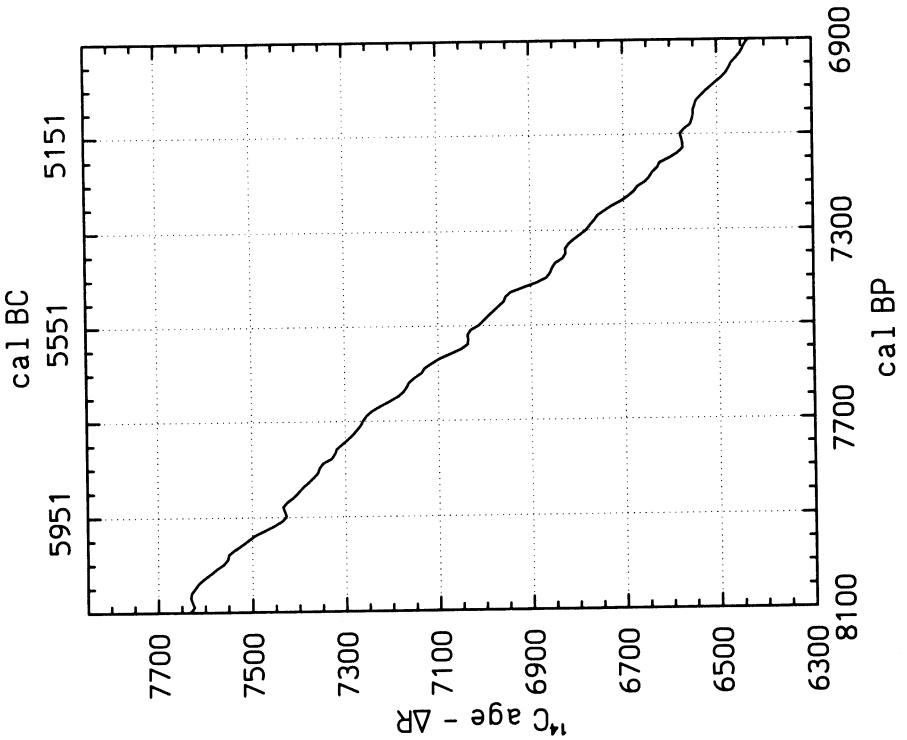

Fig. B12

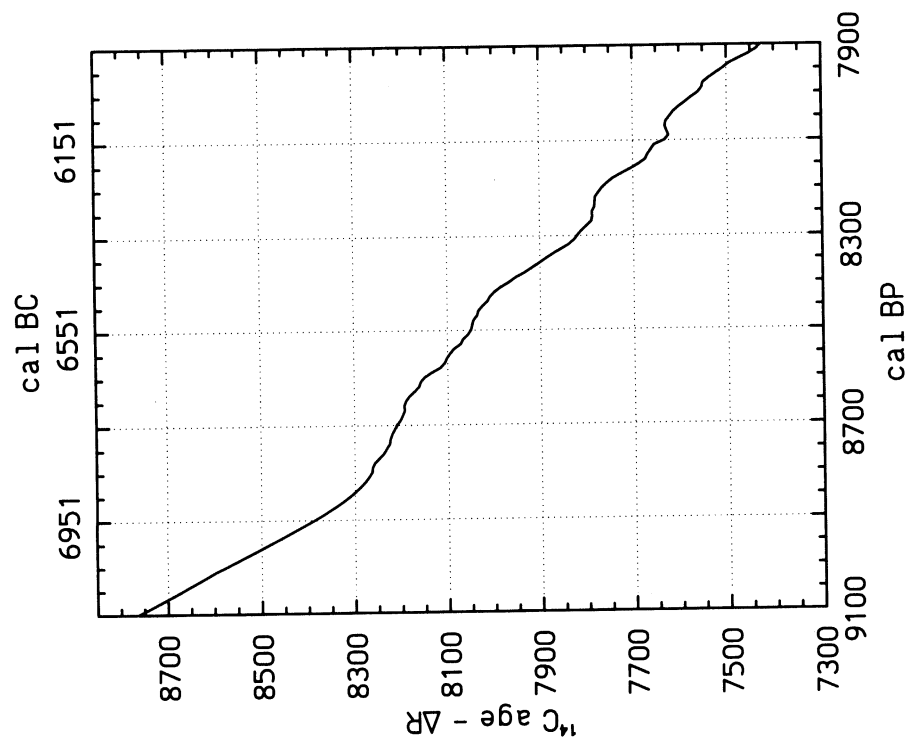

Fig. B11

https://doi.org/10.1017/S0033822200019123 Published online by Cambridge University Press

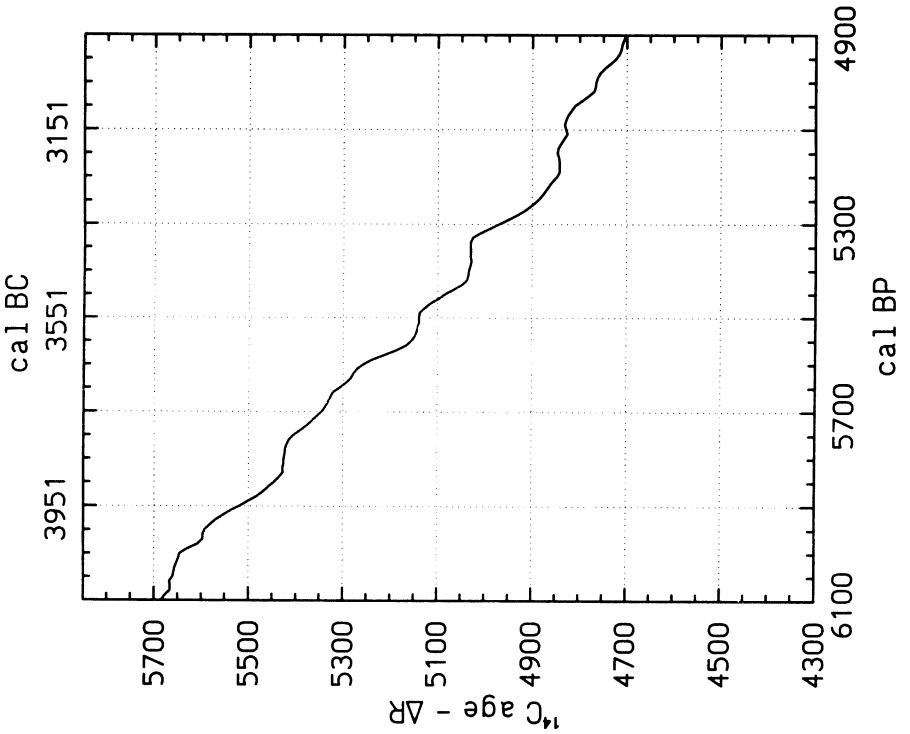

Fig. B14

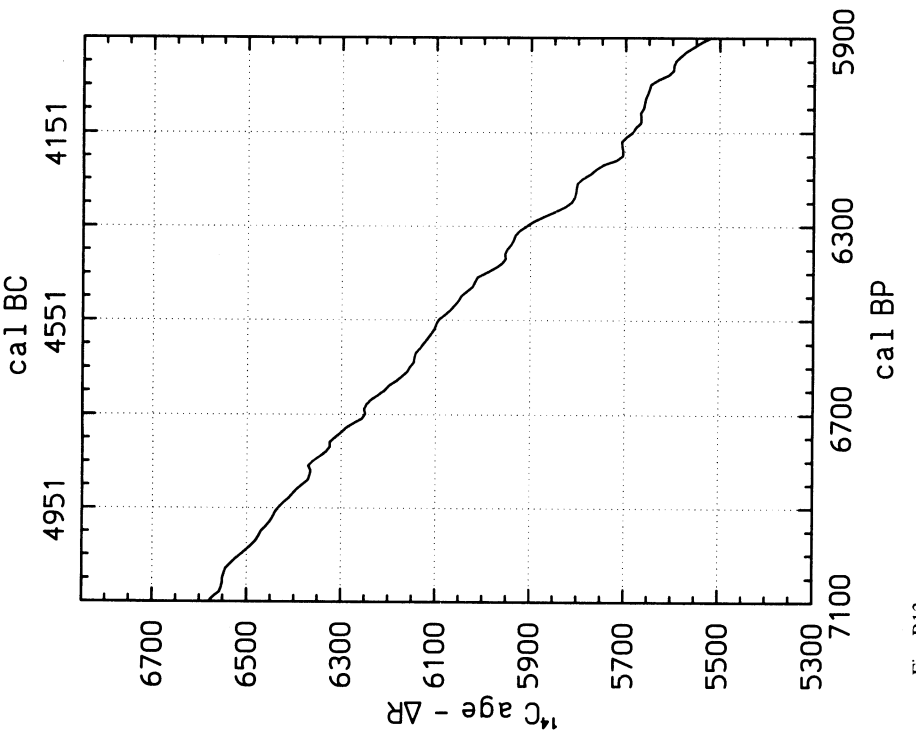

Fig. B13

https://doi.org/10.1017/S0033822200019123 Published online by Cambridge University Press

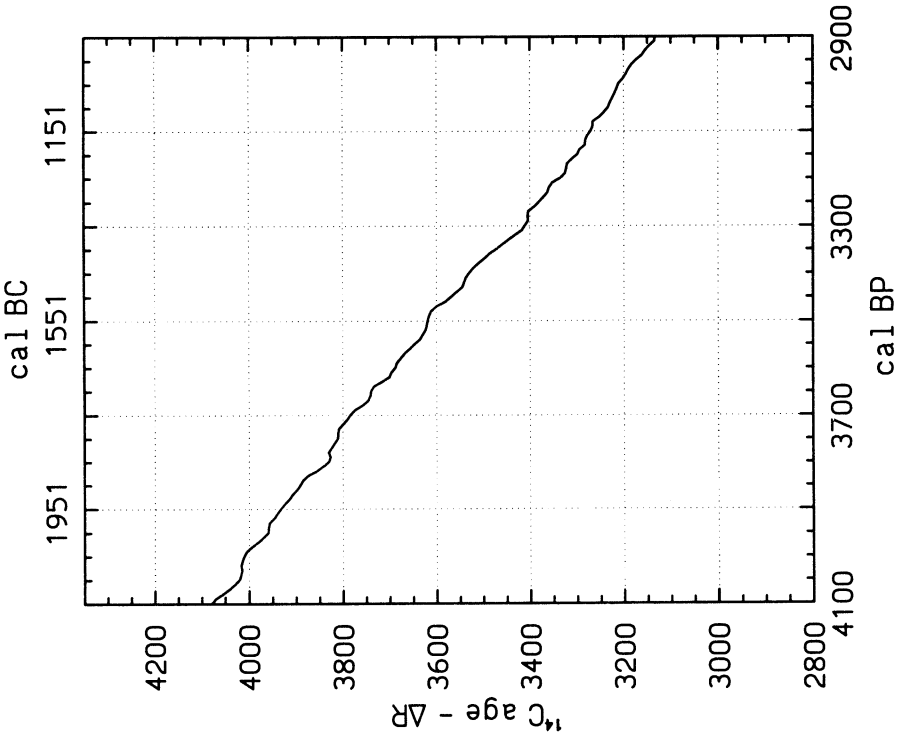

Fig. B16

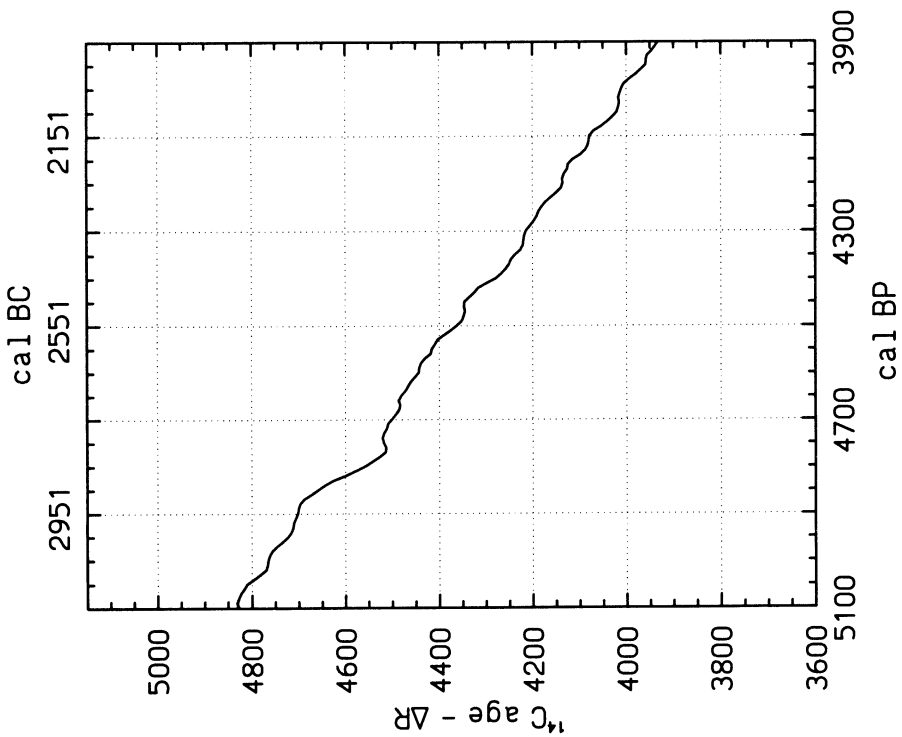

Fig. B15

https://doi.org/10.1017/S0033822200019123 Published online by Cambridge University Press

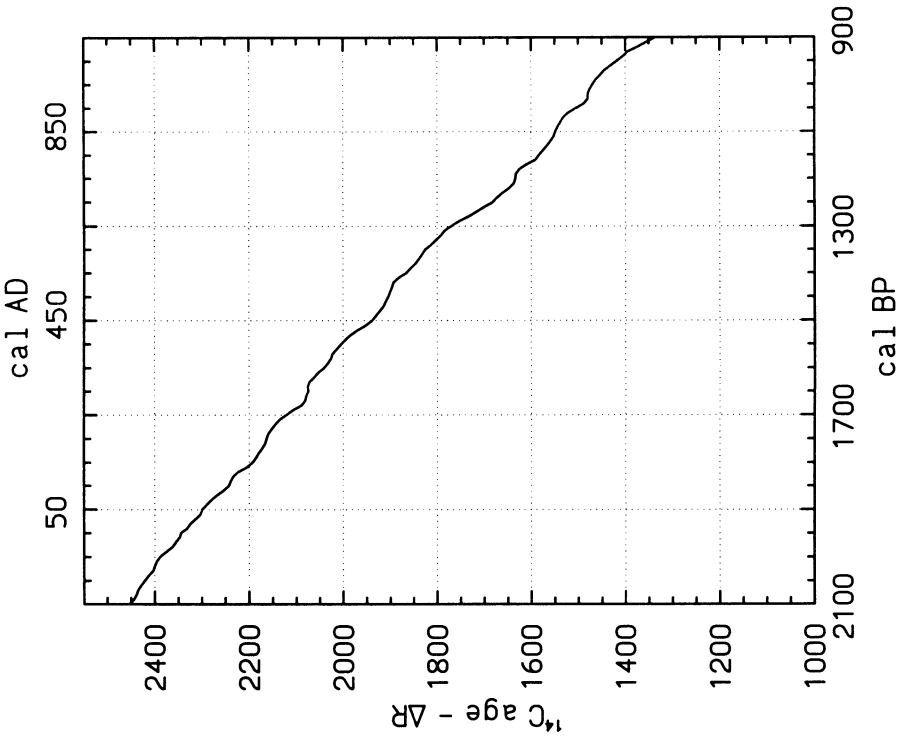

Fig. B18

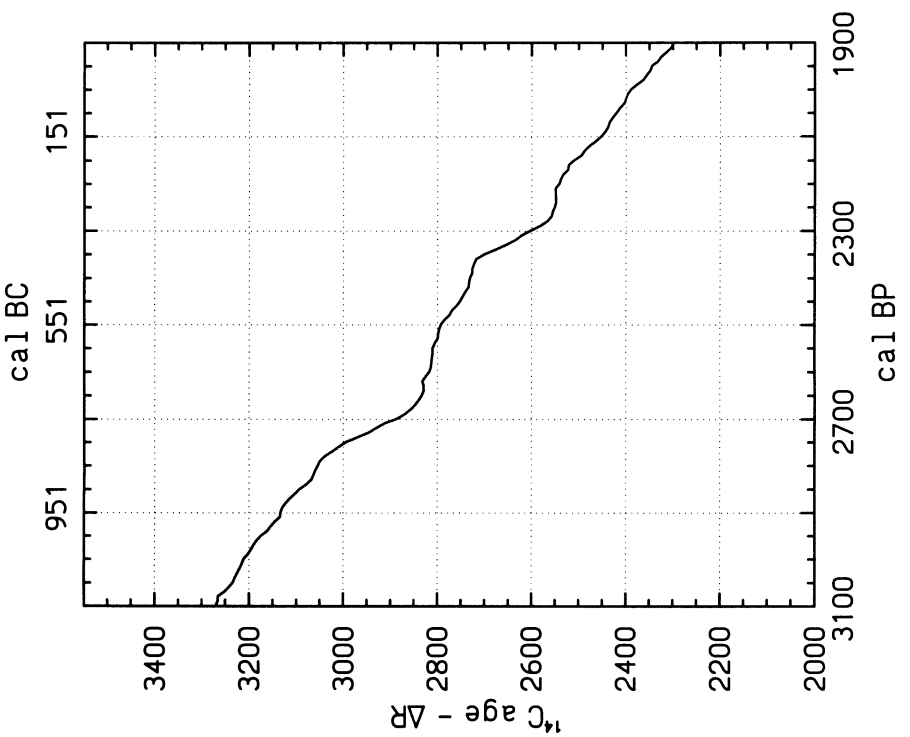

Fig. B17

https://doi.org/10.1017/S0033822200019123 Published online by Cambridge University Press

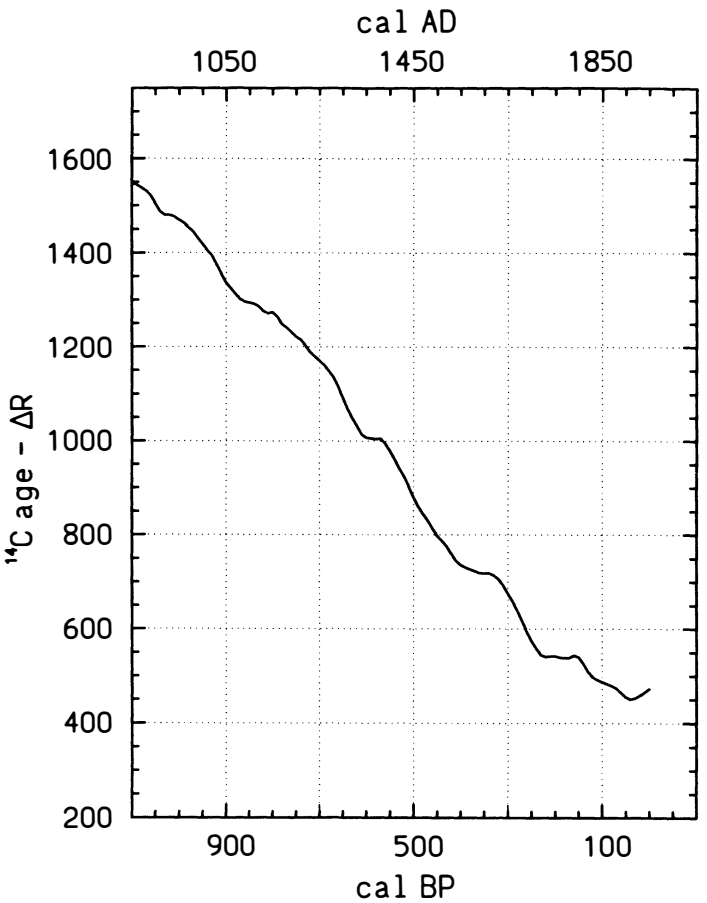

Fig. B19

https://doi.org/10.1017/S0033822200019123 Published online by Cambridge University Press